Sudan University of Science and Technology

College of Graduate Studies

كلية الدراسات العليا

Mapping of Basic Elements of Crude Oil Samples Collected from Different Oilfields in Sudan by using Laser Induced Breakdown Spectroscopy Technique

تخريط العناصر الأساسية لبعض أنواع حقول البترول الخام بالسودان بواسطة استخدام تقنية الانهيار الطيفي المستحث بالليزر

A thesis submitted for the fulfillment of the requirements for the degree of Doctor of Philosophy in Laser Applications in physics

By:

Hiba Jaafer Alamin

Supervised by:

Prof. Dr. Abdelmoneim M. Awadelgied

2019

الآية

بسم الله الرحمن الرحيم

(اللَّهُ لَا إِلَٰهَ إِلَّا هُوَ الْحَيُّ الْقَيُّومُ ۚ لَا تَأْخُذُهُ سِنَةٌ وَلَا نَوْمٌ ۚ لَّهُ مَا فِي السَّمَاوَاتِ وَمَا فِي الْأَرْضِ ۗ مَن ذَا الَّذِي يَشْفَعُ عِندَهُ إِلَّا بِإِذْنِهِ ۚ يَعْلَمُ مَا بَيْنَ أَيْدِيهِمْ وَمَا خَلْفَهُمْ ۖ وَلَا يُحِيطُونَ بِشَيْءٍ مِّنْ عِلْمِهِ إِلَّا بِمَا شَاءَ ۚ وَسِعَ كُرْسِيُّهُ السَّمَاوَاتِ وَالْأَرْضَ ۖ وَلَا يَئُودُهُ حِفْظُهُمَا ۚ وَهُوَ الْعَلِيُّ الْعَظِيمُ)

سورةالبقرة (225)

I

Acknowledgement

Thank to my supervisor for his help and support throughout the entire time we've worked together.

Also special thanks for Dr.Khalid M.Haron in Zaiem Alazhari University and Dr. Abd Alsakhi in Neelain University.

I need to send special thanks to my family my Husband for their support and help me all the time.

DEDICATION

To my Mother

My Father

My Husband

My Sisters and Brothers

Abstract

This research aim to use modern scientific technique which is laser induced breakdown spectroscopy to identify the components of some crude oil samples.

This technique was selected in this work due to its unique characteristics in terms of ease, speed and no sample preparation.

Three samples of crude oil were used in this work, collected from different locations in Sudan: Rawat, (White Nile), Melut (Upper Nile- Jonglei) and Hadida (East Darfur).

These samples was irradiated by Nd:Yag laser at 1064 nm , pulse duration10 ns , RR2Hz, with pulse energies of 120,150,170 and 190 mJ.

The result was analyzed by using atomic spectra data base (ASD) from national institute of standard and technology (NIST) and showed considerable amount of the main elements in crude oil (C, H, N, O and S) in all three samples with different ionization stages due to the different in laser energy pulse. Also transition metals such as Fe, Ti, Sc, V, Co, Mn, Ni, Cr, Cu and Mo.

Earth metals like Al, Th and B also were appeared. In addition to heavy elements like Hg, Cd was finding.

Also the spectra of the samples showed light elements such as He, Li, gaseous elements like Ar, Ne, Cl in addition to Alkali elements Ca, Na, Cs, K, Ba and Mg.

The spectra due to trace elements such as Zn, Si, P,U, Ga were recorded using this technique.

The obtained results showed that the crude oil samples has many elements and varies from one field to another in relation to the change in the age, depth and location of the well.

This work illustrated that LIBS technique was useful when apply to liquid sample and for hazard (flammable) samples like crude oil with reasonable detection limit and no sample preparation.

المستخلص

هذا البحث يهدف الى استخدام تقنية علمية حديثة وهي الانهيار الكهربائي المستحث بالليزر (LIBS) لتحديد مكونات بعض عينات من البترول الخام .

تم اختيار هذه التقنية فى هذا البحث نسبة لخواصها المتفردة من حيث الدقة والسهولة والسرعة وكذلك لا تحتاج لتحضير مسبق للعينات .

أستخدمت في هذا البحث ثلاث عينات من البترول الخام تم الحصول عليها من مناطق مختلفة في السودان : الراوات (النيل الابيض) حديدة (شرق دار فور) ومليط (اعالي النيل- جونقلي).

هذه العينات تم تشعيعها بواسطة ليزر Nd-YAG عند طول موجي 1064 nm ومعدل تكرار 2Hz وفترة نبضية 10 ns بطاقة ليزر نبضية عند 120, 150, 170 and 190 mJ

تم تحليل النتائج بواسطة استخدام أطياف قاعدة البيانات الذرية (NIST- ASD) وأظهرت كميات مقدرة من العناصر الاساسية في البترول الخام مثل الكربون , الهيدروجين , الاوكسجين , النيتروجين , الكبريت في كل العينات الثلاث بمراحل تأين مختلفة بسبب الاختلاف في الطاقة المشععة لها. كذلك ظهرت بعض العناصر الانتقالية مثل Fe, Ti, Sc, V, Co, Mn, Ni, Cr, Cu, Mo.

سجلت نتائج البحث ظهور عناصر ارضية مثل Al, Th and B بالاضافة الي بعض العناصر الثقيلة مثل Hg, Cd.

كما كشفت نتائج التحليل عن بعض العناصر الخفيفة مثل الهيدروجين , الهيليوم والليثيوم وعناصر غازية مثل الارجون والنيون بالاضافة الي بعض المعادن القلوية مثل البوتاسيوم والكالسيوم والصوديوم والمغنيسيوم والسيزيوم والباريوم . كذلك وجدت اطياف عناصر اخرى مثل Zn, Si, P, U, Ga.

أظهرت النتائج المتحصل عليها أن البترول الخام يحتوي على العديد من العناصر المختلفة وتختلف كل عينة عن الاخرى في عناصرها لعدة عوامل مثل اختلاف المنطقة التي اخذت منها العينة وعمق وعمر حقل البترول .

أظهر هذا البحث فائدة استخدام تقنية LIBS للعينات السائلة دون الحاجة لتحضير العينة وكذلك للمواد القابلة للاشتعال بدقة مناسبة .

List of Contents

Title	Page No.

List of Tables

List of Figures

Chapter One

Introduction

1.1   Introduction:

Spectroscopy is the studying of the properties of matter through its interaction with different frequency components of the electromagnetic spectrum i.e. interaction of light with matter [1].

There are two distinct aspects of this interaction that can be used to learn about atoms and molecules. One is the identification of the specific wavelengths of light that interact with the atoms and molecules [2].

The other is the measurement of the amount of light absorbed or emitted at specific wavelengths. Both determinations require separating a light source into its component wavelengths. Thus, a critical component of any spectroscopic measurement is breaking up of light into a spectrum showing the interaction of light with the sample at each wavelength.

Interactions are light that is absorbed by the atoms and molecules in the sample and light that is emitted after interacting with the atoms and molecules in the sample.

An example of spectroscopy is Infrared spectroscopy which is particularly useful for studying the vibration of bonds between carbons, hydrogen, oxygen and nitrogen atoms that predominate in organic compounds. Thus, infrared spectroscopy is a key tool of the organic chemist. Infrared spectra can indicate the presence of particular functional groups in unknown organic compounds by the presence of characteristic features.

Also Visible light spectroscopy is useful for studying some organic compound and elements that have electrons in d-orbitals, such as transition metals.

Ultraviolet spectroscopy is useful for studying some organic compounds and most biological samples. All proteins have useful ultraviolet spectra as do

nucleic acids. Furthermore, UV spectroscopy can be used to follow biochemical reactions and this tool is commonly found in biochemical laboratories. In clinical laboratories, ultraviolet spectroscopy is often the means for making quantitative determinations on plasma and urine samples [2].

In this work new promising technique which is Laser-induced breakdown spectroscopy (LIBS) was used. LIBS are an atomic emission spectroscopy technique which uses highly energetic laser pulses to estimate optical sample excitation. The interaction between focused laser pulses and the sample creates plasma composed of ionized matter. Plasma light emissions can provide "spectral signatures" of composition of many different kinds of materials in solid, liquid, or gas state. LIBS can provide an easy, fast, and accurate in situ quantitative analysis with a reasonable precision, detection limits, and cost, additionally, as there is no need for sample preparation [3].

In LIBS, at a certain energy (characteristic for each matrix) exceeding the material's breakdown threshold, the sample becomes dissociated, atomized and partially ionized to form high-temperature and high electron-density plasma. This micro-plasma may be analyzed by optical emission spectrometry. Spectrally and temporally resolved detection of the specific atomic emission will reveal analytical information about the elemental composition of the sample. Laser induced breakdown spectrometry is chiefly performed in air at atmospheric pressure, because working in a vacuum hinders one of the main LIBS advantages: easy sample-handling [4].

LIBS is useful in a wide range of fields, namely, those which can benefit from a quick chemical analysis at the atomic level, without sample preparation, or even in the field.

LIBS were used to determine the components of crude oil samples. Petroleum means rock oil, Petroleum is oily, flammable, thick dark brown or greenish

liquid that occurs naturally in deposits, usually beneath the surface of the earth; it is also called as crude oil [5].

The crude oil is a naturally occurring, unrefined petroleum product composed of hydrocarbon deposits and other organic materials e.g. (C, H, N, S and O). It is a nonrenewable resource, which means that it can't be replaced naturally at the rate we consume it i.e. limited resource.

Under surface pressure and temperature conditions, lighter hydrocarbons methane, ethane, propane and butane exist as gases,

while pentane and heavier hydrocarbons are in the form of liquids or solids [6].

Petroleum is not a uniform material. In fact; the precise chemical composition of petroleum can vary with the location and age of the field in addition to any variations that occur with the depth of the individual well. Two adjacent wells may even produce petroleum with very different characteristics.

1.2 Aim of this work:

The aim of this work is to use modern scientific method Laser induced breakdown spectroscopy (LIBS) to determine the components of some different crude oil in Khartoum collected from different locations (oil fields) in Sudan. And to reveals the advantages of using the LIBS techniques in petroleum industry because there are a many uses of crude oil that affects our lives.

1.3 Methodology:

In this work, the experimental of LIBS consisted of Nd: YAG laser with wavelength 1064 nm, pulse duration 10ns, Pulse Energy (120, 150 170 and 190)

mJ, and repetition rate 2 Hz; Ocean Optics spectrometer model USB 2000+ of detector range (200 to 1100)nm, connected with PC were used . The optical emission of laser-induced plasma was collected by fiber optic at an angle of 90^0 to the laser pulse. The glass cell used to put the samples inside it.

A laser pulse with (120, 150, 170 and 190) mJ energy was focused on the Crude Oil sample, then irradiated with these energies and the spectrum of the emitted plasma was recorded. The resulted emission spectrum was analyzed using NIST –ASD and Origin pro 9 data analysis software.

1.4 Thesis layout:

Chapter one contain an introduction and the aim of this work, research problem, and methodology and thesis layout.

Chapter two illustrates the descriptions of Laser Induced Breakdown Spectroscopy techniques, principles, applications, advantage and disadvantage of LIBS technique and literature review was presented.

Chapter three consist of experimental setup, LIBS components (Nd-YAG laser-Spectrometer-Fiber optic), also includes sample collection and preparation.

Chapter four: include the results, discussion, conclusion and recommendations.

Chapter two
Theoretical background

2.1 Introduction:

In earlier studies, the power of laser was demonstrated soon after its invention when a focused laser beam produced a bright flash in air. Another spectacular effect involved the production of luminous clouds of vaporized material blasted from a metallic surface and often accompanied by a shower of sparks when the laser was focused on a metal surface. These laser effects have found many technological applications in the fields of metal working, plasma production and semi-conductions.

Laser-induced breakdown spectroscopy (LIBS), sometimes called laser spark spectroscopy (LSS) or laser-induced plasma spectroscopy (LIPS) because it is produce from the direct detection of atomic emission of the Plasma, and it developed rapidly as an analytical technique.

This phenomenon has opened up applications in many fields of science from thin film deposition to elemental analysis of samples. The possibility of using a high power, short- duration, laser pulse to produce a high temp, high- density plasma was pointed out by Basov and Krokhin as a means of filling a fusion device by vaporizing a small amount of material [7].

Emission spectroscopy   is used for elemental analysis of targets from which the lumen as plasma is generated and can also be applied to determine the temp, electron density and atom density in the LIBS.

The current developments of this technique can be traced to the work of RadziensKi and Cremers and their co-workers in 1980, It was this research group that first coined the acronym LIBS.

In order to obtain a reliable quantitative elemental analysis of sample using LIBS, are needs to control several parameters that can strongly affect the

measurements. Some of these parameters are the laser wavelengths, its irradiance (power per unit area), the morphology of the sample surface, the amount of ablated and vaporized sample and the ability of the resulting plasma to absorb the optical energy [7].

2.2 Crude oil:

Crude oil is a mixture of comparatively volatile liquid hydrocarbons (compounds composed mainly of hydrogen and carbon), though it also contains some nitrogen, sulfur, and oxygen and trace amounts of metals such as Fe, Ni, Cu and V, Vanadium and nickel are present in large quantity in heavy crude oils.

Those elements form a large variety of complex molecular structures, some of which cannot be readily identified.

Crude oils are customarily characterized by the type of hydrocarbon compound that is most prevalent in them: paraffins, naphthenes, and aromatics. Paraffins are the most common hydrocarbons in crude oil; certain liquid paraffins are the major constituents of gasoline (petrol) and are therefore highly valued. Naphthenes are an important part of all liquid refinery products, but they also form some of the heavy asphaltlike residues of refinery processes. Aromatics generally constitute only a small percentage of most crude. The most common aromatic in crude oil is benzene.

Crude oil also is categorized as "sweet" or "sour" depending on the level of sulfur, which occurs either as elemental sulfur or in compounds such as hydrogen sulfide. Sulphur is the third most abundant constituent of crude oil. Generally, the heavier the crude oil, the greater its sulfur content. Excess sulfur is removed from crude oil during refining, because sulfur oxides released into the atmosphere during combustion of oil are a major pollutant [8].

2.3 Principles of LIBS:

LIBS technique is a powerful tool for in-situ elemental measurements in different surroundings such as vacuum, and then gas and liquids at different ambient pressures (usually performed in the atmospheric environment). The technique is based on plasma generation by an intense laser pulse, which duration is in nano-second range or shorter. When analyzing the gasses or bulk liquids, the laser pulse generates a breakdown in the media. In the case of solid samples, the plasma is produced through laser-induced evaporation of the surface layer. In both cases, the intense laser pulse is also responsible for atomization and ionization of the material.

The plasma growth and decay lead to different processes such as: expansion: shock waves formation continuum (Bremsstrahlung) emission and light absorption by free electrons (inverse Bremsstrahlung); collisions in the gas cloud with excitation and relaxation of atoms/ions; chemical recombination and, as important for LIBS, de-excitation of the species (atoms, ions and molecules) through emission of the radiation. Detection of the latter emission, obtained after Laser-induced plasma formation, is a principle of LIBS technique. This radiation is usually detected in the spectral range covering near UV, visible and near IR. Initially, the plasma temperature is very high, typically above 15000 K, and its radiation is dominated by the continuum component. Due to bremmstrahlung emission from free electrons and ions, electrons recombination the continuum emission is higher for the measurements in more dense medium (high gases pressure or inside liquids), and has a relatively fast decay.

It is followed by appearance of the ionic and atomic lines, where the ionic lines are more intense in the early plasma stage characterized with a higher temperature. Due to the high electron density in the early plasma, lines emissions are strongly collisional broadened thus not allowing to resolve emission lines from most elements in the plasma. Often the progressively

decaying plasma emission is still detected after few tens of microseconds from laser pulse. In sufficiently cooled plasma, the emission from the molecules, formed from the species initially present in the plasma, can be also detected.

Some molecules or fragments such as CN can be observed also for the shorter acquisition delays. In order to avoid that, the initial strong continuum masks emission line, and/or that the strong initially broadened lines cover the weaker lines, it is preferable to delay the spectral acquisition with respect to the Laser pulse. The acquisition gate and delay in certain experimental conditions can be optimized for obtaining maximum Signal- to-Noise Ratio (SNR) for a range of the analytical lines.

The atomic and ionic lines once assigned to specific transitions given in databases [National Institute of Standards and Technology], allow for a qualitative identification of the species present in plasma and consequently of the elements initially present in the sample. The relative intensities of the emission lines can be used for the quantitative determination of the corresponding elements.

2.4 LIBS Instruments:

The main components in any LIBS system are:

* Pulse laser that generates plasma.

* Focusing optics for the laser beam.

* Sample holder, and a sample container (ablation chamber) to house the samples in an inert gaseous environment, under a vacuum, or simply in air.

* Spectrometer for light dispersion, equipped with a detector- usually CCD device is used with or without an intensifier (ICCD).

* Optical system for collecting the emission and transporting it to a spectrometer. It can contain lenses, mirrors and fiber optics.

* Computer and electronics for triggering the laser, synchronization with the detector, for data acquisition and storage.

A short duration laser pulse of sufficient energy focused onto the surface of a material sample instantly increases its temperature above the vaporization temperature, regardless of the type of material, and generates transient high density plasma as the laser intensity exceeds (the breakdown threshold of the material 1 to 10 MW/cm^2).

 Compared with the rate of energy delivery from the laser pulse, the energy dissipation through vaporization is relatively slow and the underlying layer of material reaches critical temperatures and pressures before the surface layer vaporizes, which forces the surface to explode. Generally, material ablation and plasma formation take place during the initial period of the laser pulse, whereas rest of the laser energy is absorbed by the ablated material to form luminous plasma. The temperature of the plasma emitting UV and visible radiation is in the range of $10^4 - 10^5$ K, whereas the electron number density ranges from 1015 to 1019 cm^{-3} and the plasma-plume may last from a few microseconds to several seconds.

 Various lasers with wavelengths ranging from IR to UV regions have been used in LIBS. These include solid-state lasers such as the Nd: YAG laser (1064 nm, 532 nm and a pulse duration of 5 to10 ns); and the ruby laser (693 nm, and a pulse duration of 20 ns); gas lasers such as the CO_2 laser (10^{-6} nm, and a pulse duration of 100 ns), and the N_2 laser (337 nm, and a pulse duration of 30 ps to 10 ns); and excimer lase rs (193 nm [ArF], 248 nm [KrF], 308 nm [XeCI], and a pulse duration of 10–20 ns). Among all these, Nd: YAG lasers are the most widely used.

The typical output energies for these lasers are tens of mJ to hundreds of mJ per pulse, and peak power is in the range of MW. These laser beams are focused to spots few tens of micrometers in diameter producing $10^{10} - 10^{12}$ W/cm^2 irradiance. The characteristics of a laser, such as energy, energy stability, wavelength, pulse duration, beam quality, and mode quality, together with the properties of the target material, affect the production and characteristics of the plasma. Typically, 100 mJ/ pulse energy is sufficient to generate plasma for the analysis of most of the materials [7].

2.4.1 Lasers:

The main device of LIBS is the laser. It generates the energy to induce the plasma and mainly determines the plasma features. The main parameters related to the laser are the pulse time, the energy per pulse, the wavelength, and the number of pulses per burst. Obviously, each application works better with a combination of these parameters. For example: Nanosecond-pulsed lasers are the most common for LIBS.

Laser Wavelength: The wavelength influence on LIBS can be explained from two points of view; the laser-material interaction (energy absorption) and the plasma development and properties (plasma-material interaction).

When photon energy is higher than bond energy, photon ionization occurs and non-thermal effects are more important. For this reason, the plasma behavior depends on wavelength in nanosecond LIBS setup. In the same way, the optical penetration is shorter for UV lasers, providing higher laser energy per volume unit of material. In general: the shorter the laser wavelength, higher the ablation rate and the lower the elemental fractionation [9].

The plasma ignition and its properties depend of wavelength. The plasma initiation with nanosecond lasers is induced by two processes; the first one is inverse Bremsstrahlung by which free electrons gain energy from the laser

during collisions among atoms and ions. The second one is photoionization of excited species and excitation of ground atoms with high energies.

For short wavelengths (between 266 and 157 nm) the photoionization mechanism is more important. For this reason, the shorter the wavelength in this range, the lower the fluency necessary (energy per unit area) to initiate ablation. In addition, when inverse Bremsstrahlung occurs, part of the nanosecond laser beam reheats the plasma. This increases the plasma lifetime and intensity. Longer wavelengths increase inverse Bremsstrahlung plasma shielding, but reduce the ablation rate and increase elemental fractionation (elemental fractionation is the redistribution of elements between solid and liquid phases which modifies plasma emission).

The most common laser used in LIBS is pulsed Nd:YAG. This kind of laser provides a compact, reliable, and easy way to produce plasmas in LIBS experiments. The fundamental mode of this laser is at 1064 nm and the pulse width is between 6 and 15 ns. This laser can provide harmonics at 532, 355, and 266 nm, which are less powerful and have shorter time pulses (between 4 and 8 nm). The fundamental and the first harmonic are the most common wavelengths used in LIBS. This harmonics can be useful to work with different wavelengths in the same environmental conditions, because a lot of Nd:YAG lasers can produce all of them. Other kinds of lasers can be used in LIBS, such as CO_2 or excimer lasers to work in far IR or UV ranges, respectively.

Laser Energy: The energy parameters related with laser material interaction are fluence (energy per unit area,) and irradiance (energy per unit area and time,). Ablation processes (melting, sublimation, erosion, explosion, etc.) have different fluence thresholds. The effect of changes in the laser energy is related to laser wavelength and pulse time. Hence, it is difficult to analyze the energy effect alone. In general, the ablated mass and the ablation rate increase with laser energy [9].

Acquisition Time and Delay:

The first stages of LIBS-induced plasma are dominated by the continuum emission. The time gate of decay of this continuum radiation change with a wide range of experimental parameters, such as laser wavelength and pulse time, ambient pressure or sample features. Besides, these experimental parameters fixes set the time periods of atomic emission, the most interesting stage of LIBS plasmas.

For Nd:YAG lasers, both times for gate delay and gate window are in the order of microseconds.

2.4.2 Spectrometers and Detectors:

The spectrometer or spectrograph is a device which diffracts the light emitted by the plasma. There are different designs, such as Littrow, Paschen-Runge, Echelle, and Czerny-Turner. The Czerny-Turner spectrograph is the most common device in LIBS. This spectrograph is composed of an entrance slit, two mirrors, and a diffraction grating. The light comes through the slit and reaches the first mirror which collimates the light, directing it onto the grating. Light is reflected at different angles according to its wavelength. The second mirror focuses the light on the focal plane where the detector is placed.

In recent years, the Echelle spectrograph has been used more extensively. The Echelle spectrograph uses a diffraction grating placed at a high angle, producing a large dispersion in a small wavelength range in each order. As the orders are spatially mixed, a prism is used to separate them. The orders are stacked vertically on the focal plane. For that reason, Echelle devices need a two-dimensional detector. Each vertical portion of the detector contains a part of the spectra and the software composes the whole spectrum.

Different kinds of detectors are used in LIBS, depending of the application. To measure light intensity without spectral decomposition, the photomultiplier tube (PMT) or avalanche photodiode (APD) can be used. On the other hand, for one-dimensional spatial information, the researcher can combine a spectrograph and a photodiode array (PDA) or an intensified photodiode array (IPDA) for time-resolved measurements.

If two-dimensional spatial information is required, the most common devices are charge coupled devices (CCD) and intensified CCD (ICCD). A CCD detector provides less background signal, although ICCD improves the signal-to-noise ratio and is better for time-resolved detection using windows of a few nanoseconds [9].

2.4.3 Fiber optics:-

Laser beam, sometimes expanded, is focused onto a sample by means of one or more focusing lens. Focal length of the system must provide a sufficiently small laser spot, i.e. the sufficient laser energy density for the plasma generation, e.g for underwater LIBS applications a short focal length must be used (20-30 mm) due to the high water absorption and light scattering by suspending particles.

A mono-axial system is often used the beam usually passes a pierced mirror to deflect the plasma radiation towards the detection system. Also it is less sensible to misalignment which recommended for analysis of irregular surfaces such as rocks and soil.

For most of the sample types, the elemental emission lines in UV spectra supply a lot of analytical information, so the collecting optical system should be transparent in this spectral range. In these cases quartz optics is usually employed.

Typical collecting system contains an optical fiber serves to split signal towards the entrances of spectrometer. Echelle spectrometers have an entrance for a circular fiber with aperture up to 50 μm diameter.
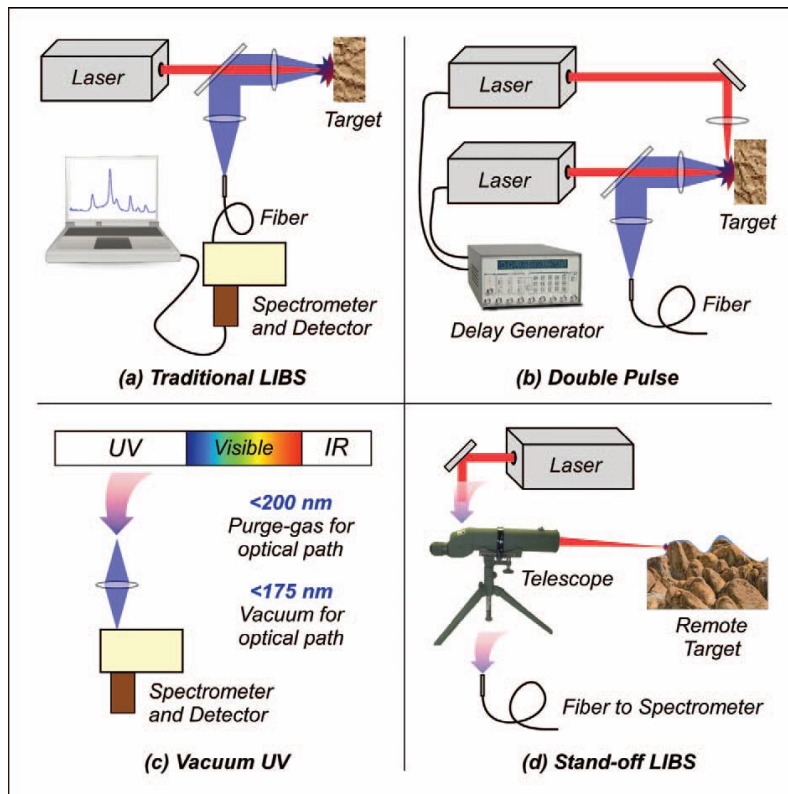
Fig (2.1): LIBS experimental setup.

Figure (**2.1**) shows the experimental LIBS setup. (a) A ''traditional'' setup, consisting of a single laser focused with a spherical lens close to the target position and axial collection of the plasma radiation with a pierced mirror and a spherical lens to form an image of the plasma on the entrance of a fiber optic optically coupled with the mono-chromator. (b) Double-pulse LIBS setup in an orthogonal configuration. The delay generator controls the delay between the two pulses. With this arrangement, both pre-spark and re-heating of the plasma can be chosen. (c) Photon collection can be accomplished in the vacuum UV as well as in the IR regions. Purging of the optics with nitrogen is useful for measurement below ~200 nm and down to ~175 nm, while below ~175 nm, vacuum operation is necessary. (d) Stand-off configuration. The plasma radiation is collected by the telescope and sent to the spectrometer via fiber optic [10].

A focused pulsed laser hits the sample removing a very small amount of material from the surface. The sample is hit by thousands of pulses during a typical one-second measurement. The material is heated up to and exceeding 10,000 degrees Celsius. The temperature is so high that the atoms actually break up and form the plasma.

When the high power pulsed laser hits the sample, the electrons in the outer shells are ejected. Because electrons in the outer shells are shielded by the inner shell electrons, they aren't strongly drawn by the nucleus.

The ejected electrons create a vacancy, making the atom unstable. When the pulse stops, the plasma starts to cool down and the vacancy is filled by electrons cascading down from the outer electron shells. The excess energy released when the electrons move between two energy levels or shells is emitted in the form of element specific light.

For a typical metallic sample containing iron, manganese, chromium, nickel, vanadium, and so on, each element emits many wavelengths leading to a spectrum of up to thousands of peaks.

The wavelengths of light are collected through a fiber optic cable and then processed by the spectrometer.

Each element is associated with a specific spectral peak. LIBS spectra are quite complex with potentially hundreds or even thousands of lines for each element.

The concentration of the element is calculated from the intensity of the spectrum peak. Then an advanced algorithm is used to identify the sample type and calculate the concentrations [11].

The plasma spectrum contains emission from the continuum component, the atomic, ionic and molecular spices. The number of detected lines depends on the corresponding element concentration in the sample. Due to the spectral interferences, it is important to use high- resolution spectrometers, a 0.1 nm or better is typical for the LIBS systems.

In the case of a low resolution system the loose of analytical information is clear, this allows for the detection of main sample constituents but rarely for minor and trace elements due to the spectral overlap of different lines.

In the early days, a photographic plate was used as a detector which had the advantage of wide wavelength range with relatively low cost but had the disadvantage of being time consuming with low reproducibility. Photographic detection has been gradually replaced by detectors for spectrally resolved emission such as a photomultiplier tube (PMT), a photodiode array (PDA), or a charge-coupled device (CCD) which provide fast and accurate measurements [7].

 The CCD is usually operated in full vertical binning, in this way spatial light distribution along the slit is lost, but much higher signal is obtained due to vertical (parallel to the slit) signal integration across the pixels.

The spectrometer entrance slit must be small with diameter up to 0.05 mm, to reduce signal collection efficiency as a large portion of the plasma is imaged out of the slit aperture, directly or through an optical fiber.

Long duration measurements runs require the spectrometer thermal stabilization, since the small temperature variations can cause a shift between different diffraction orders.

There are various detection systems, such as mass spectrometry (MS), atomic emission spectrometry (AES), atomic absorption spectrometry (AAS), and laser excited atomic fluorescence spectrometry (LEAFS).

2.5 Applications of LIBS:

The technological developments leading to the emergence of broadband high-resolution spectrometers has led LIBS into the 21st century with unprecedented capabilities to extract spectral information from micro-plasmas. It is now possible to detect almost all chemical elements in the periodic table by analyzing the UV, visible and IR emission prevalent in laser-generated sparks.

The use of femtosecond laser pulses in LIBS experiments has led to better precision and better reproducibility in emission measurement as compared to nanosecond pulses. This improvement is attributed to high peak powers. Femtosecond lasers consistently create well-defined craters and lead to better ablative reproducibility than nanosecond lasers. Extremely short fs-laser pulses account for some remarkable features as atomizers. In contrast to ns-lasers, the impact of the fs-laser energy on the sample has ceased before the plasma is formed. There is no shielding by the plasma and hence no dissipation of laser energy by it. The ablation threshold is lower than for ns-lasers and the energy is more localized in the sample leading to better spatial resolution [7].

2.5.1 LIBS Application to Off-Gas Measurement:

LIBS measurements of off-gas have a wide range of applications from the process control of a production plant to thermal waste treatment process. The detection of trace metals in the off-gas of various industrial plants such as coal-fired power plants, cement kilns, incinerators are a great public-health and environmental concern.

LIBS can perform off-gas measurements by focusing the laser beam on the gas stream through a window and collecting the signal through an optical fiber.

An irradiance corresponding to electric field strength on the order of 10^5 volt/cm with a gas near atmospheric pressure can produce gas breakdown through multi-photon ionization or electron avalanche.

Beside the particle size (micron), the laser-induced gas breakdown thresholds also depend strongly on the gas pressure and the laser wavelength.

Typically, laser-induced air breakdown has a plasma temperature of 20,000 K and an electron density of $1017-1018$ cm^{-3} after the plasma is formed.

The application of LIBS for gas analysis is involved a focused high-energy pulsed laser to produce the breakdown in the gas medium. The high temperatures and electron density laser-induced plasma prepares and excites the

sample in single step. The emission from the laser plasma can be used directly to measure the composition of gas, eliminating the need for sample preparation. The experimental arrangement of the LIBS system requires a laser system that can deliver high pulse energy (e.g. 100–300 mJ/pulse) to produce a spark in the gas medium. A frequency-doubled Nd:YAG laser is directed and focused on the desired gas sample with a lens of proper focal length (generally 10–20 cm). The emission from the spark was collected with a UV optical fiber bundle and sent to the detection system. Usually one Czerny-Turner spectrometer that can cover a spectral region of 20–40 nm simultaneously is used for gas measurements. The gate delay time and gate width were adjusted to maximize the signal-to-background (S/B) and signal-to-noise (S/N) ratios, which are dependent on the emission characteristics of the elements as well as the experimental configuration [7].

2.5.2 Application for liquid samples:

The laser pulses generate bubbles (aerosols) inside liquids that are transparent at the laser wavelength. These bubbles may reach the liquid surface absorb the laser beam, change the angle of incidence between the laser beam and the liquid surface, partially prevent the laser light from reaching the sample surface and then change the characteristics of the plasma; thereby affecting reproducibility of measurement, and change the emission intensity.

To overcome these problems a variety of experimental LIBS configurations have been employed for studies of liquid surfaces, bulk liquids and liquid jets.

Cremers et, al described a method where an initial laser pulse produced a gas bubble within the water bulk, and a time-delayed second laser pulse analyzed the gas present inside the bubble. This approach resulted in an enhancement in the line intensities by a dramatic factor of 50 for oxygen line at 777.44 nm and by a moderate factor of 3 to 4 for the calcium and magnesium resonance lines, increasing the analytical sensitivity and making the bulk analysis a reasonable

option. This double-pulse plasma-generation approach has also been used by Pichahchy et al. and, Nyga and Neu in their studies on the metal composition of specimens submerged in water. Despite the evident problems of splashing in the case of surface excitation configuration, some researchers have used this approach. Berman and Wolf and Arca et al. focused the laser LIBS of Liquid Samples 225 pulse on the surface of liquid solutions and reported a minimum delay of 1–3s for detecting trace concentrations of nickel, magnesium, calcium, and chromium [7].

2.5.3 Applications for solids:

In an early study, LIBS was used for analysis of environmental solids, including soils, sands, and sewerage sludge. A considerable focus was on optimization of the LIBS technique to address crater formation and aerosol production, size effects, timing, and reproducibility.

Good calibration results were obtained for determination of heavy metal concentrations with detection limits in the 10 mg/g range. Pollution monitoring and analysis of soils has been the focus of many additional studies, including for the analysis of a wide range of toxic and heavy metals (Al, Cr, Cu, Fe, Mg, Mn, Pb, Ti, vanadium (V), and Zn) using LIBS in combination with an established laboratory-based analytical technique such as AAS, ICP-OES, GF-AAS, and ICP-MS.

 The analysis of carbon in soils remains an attractive target for LIBS. Using the 247.8-nm carbon line, LIBS was found to produce a detection limit of 300 mg/kg, a precision of 4–5%, and an accuracy of 3–14%.

The assessment of total carbon (organic and inorganic) using LIBS was examined using both unwashed and acid-washed soils, with LIBS proving useful for determination of both organic and inorganic carbon in soil.

An online LIBS instrument was successfully used for analysis of K, Na, and Mg in soil. The use of LIBS for analysis of nitrogen in soils presents a challenge due to the significant atmospheric nitrogen content and therefore the possibility for spectral interference. The potential of LIBS for nitrogen analysis in soils was investigated using both atmospheric and reduced pressures. Using the 746.8 nm N(I) line, successful calibration curves were realized at a reduced pressure of 0.04 Torr, giving a detection limit of 0.08%.

LIBS have been used rather broadly for analysis of vegetative materials, including for nutrient analysis as well as the bioaccumulation of pollutants, for example, with phytoremediation. The use of femtosecond LIBS for detection of heavy metal accumulation in leaf samples was assessed and compared directly to X-ray microradiography. Single pulse LIBS was assessed for mapping silver and copper distribution in plants and compared directly to LA-ICP-MS analysis. The analysis of the minerals such as pyrite, PbS, and zinc blende (ZnS), along with several others, was reported using LIBS at the wavelength of 370 nm.

2.5.4 Steel applications:

Steel analysis has always been a popular application for LIBS. It has been applied to multi-elemental analysis of slag samples from a steel plant. Avoiding sample preparations, liquid slag was captured in special probes, cooled, and then analyzed with LIBS, a Nd:YAG laser beam was expanded to about 70mm in diameter and then focused with a lens system. Also the Czerny-Turner spectrometer with an ICCD detector was used. Stainless steel samples were placed in the geometrical center of an oven whose door was opened for a short time for rapid measurements.

At high temperature stainless steel can lose its protecting oxide layer and accumulate superficial oxidation called scaling. The ratios of elements such as chromium to chromium plus iron, observed in a matter of minutes, presented quantitative information about the dynamic growth of the scale layer.

Depth of the scale layer was determined by the number of laser pulses required to reach the underlying matrix material [12].

2.5.5 Industrial applications:

LIBS technique for various industrial applications ranging from: process control of materials during manufacturing, to rapid sorting of scrap materials during recycling, and remote characterization of highly radioactive nuclear waste.

Areas of industry: (i) metals and alloys processing, (ii) scrap sorting and recycling. **Metals and alloys processing: e.g.** Identification of pipe fittings: different steel grades are used for the production of pipe fittings.

The range of processed materials extends from high alloy steel grades to nickel base alloys.

The light emitted from the laser-induced plasma is collected by a fiber optic cable and transferred to a Paschen–Runge spectrometer equipped with 12 photomultipliers for the elements Fe, Ni, Cr, Mo, Ti, Cu, Nb, Al, and W. For time-resolved spectrometry, the photomultiplier signals are processed by a multi-channel electronic device with fast gate able integrators and analog-to-digital converters.

Slag analysis: The composition of a steel melt is influenced by chemical reactions of the melt with slag components. Therefore the

chemical analysis of the slag provides essential information for an efficient metallurgical process control. A Q-switched Nd:YAGlaser operating at 1064 nm was used to excite the plasma. The spectrometer has a Rowland circle diameter of 500 mm. The dispersed radiation passing the exit slits is detected by photomultiplier tubes (PMT). The integrated Paschen–Runge spectrometer simultaneously detects emission lines of the relevant elements Ca, Fe, Si, Mn, Mg, Al, and Ti. Most of the lines belong to atomic transitions of the respective elements.

Analyzing liquid steel by LIBS started as early as 1965. Runge *et al*. used a ruby laser to analyze nickel and chromium of molten stainless steel samples in the laboratory.

Prototype LIBS analyzer during operation at an induction furnace with a 100 kg steel melt was used to analyze the important elements like carbon, sulfur, and phosphorus, the radiation of the laser-induced plasma is guided through a protection window, a 200 mm collimating lens (both made of MgF2) and two beam steering mirrors into a vacuum Paschen–Runge spectrometer with a Rowland circle diameter of 750 mm and the Nd:YAG laser emits pulse bursts at 10 Hz repetition rate [13].

2.6 Advantages and disadvantages of LIBS:

LIBS, like other methods of AES, have the following advantages compared with some non-AES-based methods of elemental analysis:

1. Ability to detect all elements,
2.   Simultaneous multi-element detection capability.
3. Simplicity,
4. Rapid or real-time analysis,
5. No sample preparation,
6. Allows in situ analysis requiring only optical access to the sample.
7. Ability to sample gases, liquids, and solids equally well,
8. Good sensitivity for some elements (e.g. Cl, F) difficult to monitor with conventional AES methods,
9. Adaptability to a variety of different measurement scenarios,
10. Robust plasma that can be formed under conditions not possible with conventional plasmas [13].

While the disadvantages of LIBS are:

1**.** Increased cost and system complexity.

2. Difficulty in obtained suitable standards (semi-quantitative).

3. Large interference effects (including matrix interference and, in the case of aerosols, the potential interference of particle size).

4. Detection limits are generally not as good as established solution techniques.

5. Poor precision, typically 5-10%, depended on the sample homogeneity, sample matrix, and excitation properties of the laser.

6. Possibility of ocular damage, by the high energy laser pulses [14].

2.7 Literature review:

Saifeldi n Yassin Mohamed in 2012 used Laser induced break down spectroscopy to identify the chemical characterization of crude oil and soil samples with respect to identification of constituents organic, inorganic materials and heavy metal components.

The samples were collected from Heglig Oilfield, Bamboo Oilfield, Defra Oilfield, Unity Oilfield, Adaril Oilfield, Balela Oilfield, and Hamra well. Characteristics elements (organic and inorganic materials) in petroleum such as C, H, N, O, Na, and Ca were detected. The spectra due to heavy elements in crude oil and soil samples such as Fe, Mg, Cu, Zn, Na, Ni, K, Ti, Ba, Cr, Li, Sr, Bi, Zr, Co, P and V were recorded. In addition, contributions from Ca, Si and Al were noticed. The use of intensity ratios of line and band emissions in the crude oil samples allowed a better characterization of the samples than the simple use of peak intensities. Concentration of heavy elements in the soil samples was detected using Inductively Coupled Plasma Mass Spectroscopy (ICP-MS).

The number of heavy elements detected in crude oil was: thirty element in the Adaril oilfield, twenty eight element in the Balela oilfield , twenty three element in the Bambo oilfield, fourteen element in the Diffra oilfield, eighteen element in the Unity oilfield and sixty nine element in the soil of Hamra oil well located in the Hegleg oilfield.

Concentrations of heavy metals were ranging from very high concentration e.g (Ca, K, Na, Si, Ba, F, Al, Ni, Mg and Mn) to medium concentration (Cu, Bi, Sr and Zn) and low concentration e.g. (vanadium and sulfur) were also detected [15].

In 2013 Yong He, Jiajian Zhu, Bo Li, Zhihua Wang, Zhongshan Li, Marcus Aldén, and Kefa Cen used Laser-Induced Breakdown Spectroscopy as In-situ Measurement of Sodium and Potassium Release during Oxy-Fuel Combustion of Lignite. (LIBS) was used to measure quantitatively the sodium (Na) and

potassium (K) release from burning coal particles under oxy-fuel combustion environments. A specially designed laminar premixed burner was employed to provide a post flame environment with different O2 and CO2 concentrations, in which the effects of O2 and CO2 on the release of Na and K during coal oxy-fuel combustion were studied systematically. For the de-volatilization stage, neither O2 nor CO2 had significant influence on the Na and K release. The release of Na and K during the char stage, however, changed significantly at different O2 and CO2 concentrations. Under these experimental conditions, when the O2 concentration increased from 3.9% to 10.6%, the peak concentration of Na at the char stage increased from 15.2 mg/m3 to 33.7 mg/m3, and the maximum concentration of K increased from 6.2 mg/m3 to 11.7 mg/m3. When the CO2 concentration increased from 35.8% to 69.4%, the release of Na and K was inhibited during the char stage, with the peak concentration decreasing from 8.9 mg/m3 to 6.9 mg/m3 for Na and from 3.7 mg/m3 to 2.4 mg/m3 for K. During the ash stage, the release of Na and K decreased with the O2 concentration, whereas it increased with the CO2 concentration [16].

Epuru Nageswara, Rao.. Sreedhar, Sunku.. Soma, Venugopal Rao in 2014 used the technique of femtosecond LIBS to investigate seven explosive molecules of nitro-pyrazole in three different atmospheres: ambient air, nitrogen, and argon. The FLIBS data illustrated the presence of molecular emissions of cyanide (CN) violet bands, diatomic carbon (C2) Swan bands, and atomic emission lines of C, H, O, and N.

The plasma dynamics: the decay times of molecular and atomic emissions were determined from time-resolved spectral data obtained in three atmospheres: air, argon, and nitrogen. The CN decay time was observed to be longest in air, compared to nitrogen and argon atmospheres, for the molecules pyrazole (PY) and 4-nitropyrazole (4-NPY). In the case of C2 emission, the decay time was observed to be the longest in argon, compared to the air and nitrogen

environments, for the molecules PY, 4-NPY, and 1-methy l, 3, 4, 5 - trinitropyrazole. The intensities of the CN, C2, C, H, O, and N emission lines and various molecular/atomic intensity ratios such as CN/C2, CN/C, C2/C, O/H, O/N, and N/H were also deduced from the LIBS spectra obtained in argon atmosphere. A correlation between the observed decay times and molecular emission intensities with respect to the number of nitro groups, the atmospheric nitrogen content, and the oxygen balance of the molecules was investigated. The relationships among the LIBS signal intensity, the molecular/atomic intensity ratios, and the oxygen balance of these organic explosives was also explored [17].

In 2014 M. A. Gondal, Y. W. Maganda, M. A. Dastageer, F. F. Al Adel, A. A. Naqvi, and T. F. Qahtan used LIBS system to detect of carcinogenic chromium in synthetic hair dyes. LIBS system, consisting of a pulsed 266 nm laser radiation, in conjunction with a high-resolution spectrograph, a gated intensified charge coupled device camera, and a built-in delay generator were used to develop a sensitive detector to quantify the concentration of toxic substances such as chromium in synthetic hair dyes available on the local market. The strong atomic transition line of chromium (Cr I) at 427.5 nm wavelength was used as a fingerprint wavelength to calibrate the detection system and also to quantify the levels of chromium in the hair dye samples. The limit of detection achieved by LIBS detection system for chromium was 1.2 ppm, which enabled to detect chromium concentration in the range of 5–11 ppm in the commercial hair dyes. The concentrations of chromium in the hair dyes measured were validated using a standard analytical technique such as inductively coupled plasma mass spectrometry (ICPMS), and acceptable agreement was found between the results obtained by the two methods (LIBS and ICPMS) [18].

Salvador Guirado.. J. Javier Laserna.. Francisco J. Fortes..in 2015 used a Novel Remote (LIBS) System of multi-Pulse Excitation for Underwater Analysis of Copper-Based Alloys. The use of multi-pulse excitation has been

evaluated as an effective solution to mitigate the preferential ablation of the most volatile elements, namely Sn, Pb, and Zn, observed during LIBS analysis of copper-based alloys. The novel remote LIBS prototype used in this experiment featured both single-pulse (SP-LIBS) and multi-pulse excitation (MP-LIBS). The remote instrument is capable of performing chemical analysis of submersed materials up to a depth of 50 m. LIBS analysis was performed at air pressure settings simulating the conditions during a real subsea analysis. A set of five certified bronze standards with variable concentration of Cu, As, Sn, Pb, and Zn were used. In SP-LIBS, signal emission is strongly sensitive to ambient pressure. In this case, fractionation effect was observed. Multi-pulse excitation circumvents the effect of pressure over the quantitative analysis, thus avoiding the fractionation phenomena observed in single pulse LIBS. The use of copper as internal standard minimizes matrix effects and discrepancies due to variation in ablated mass [19].

In 2015 Ahmed Asaad I. Khalil, Mohammed A. Gondal, Mohamed Shemis, and Irfan S. Khan used ultraviolet LIBS for detection of carcinogenic metals in human kidney stones extracted through the surgical operation. ND-YAG laser operating at 266 nm wavelength and 20 Hz repetition rate along with a spectrometer interfaced with an intensified CCD (ICCD) was applied for spectral analysis of kidney stones. The ICCD camera shutter was synchronized with the laser-trigger pulse and the effect of laser energy and delay time on LIBS signal intensity was investigated. The experimental parameters were optimized to obtain the LIBS plasma in local thermodynamic equilibrium. Laser energy was varied from 25 to 50 mJ in order to enhance the LIBS signal intensity and attain the best signal to noise ratio. The carcinogenic metals detected in kidney stones were chromium, cadmium, lead, zinc, phosphate, and vanadium. The results achieved from LIBS system were also compared with the inductively coupled plasma–mass spectrometry analysis and the concentration detected with both techniques was in very good agreement. The plasma

parameters (electron temperature and density) for SP–LIBS system were also studied and their dependence on incident laser energy and delay time was investigated as well [20].

Mauro Martínez†, Ryszard Lobinski‡, Brice Bouyssiere‡, Vincent Piscitelli†, José Chirinos†, and Manuel Caetano in 2015 used LIBS for determination of Ni and V in Crude Oil Samples Encapsulated in Zr Xerogels. Pellets produced from xerogels proved to be durable and homogeneous, and they allow for ablation of the samples without splatters. Ni and V present in Venezuelan crude oil were used as probe elements, and Yttrium was used as an internal standard to take into account the fluctuations in the amount of ablated material. Detection limits of 7 and 4 µg g–1 for V and Ni were estimated, respectively. The accuracy of the method was assessed by analyzing standard reference materials. The measured values of V and Ni in the SRM agreed well with the certified values at the 95% confidence level [21].

In 2015 Maria Mohammed Osman Taha used LIBS to investigate, and calculate the concentrations, the heavy metals in industrial water collected from dairy products processing plants. For this purpose, a pulsed Nd:YAG laser at 532 nm, RR 2Hz, pulse duration 10 ns, with pulse energies of 30, 60, 80, and 100 mJ irradiated on industrial water samples. Five industrial waste water samples, collected from diary product plants, were used as study samples. The emission spectra of the plasma were collected via optical fiber and analyzed by Ocean Optics LIBS 4000+ spectrometer, and the recorded spectra of the samples were analyzed using Atomic Specrta Database line (NIST) data.

The analysis of the spectra showed considerable amounts of neutral atoms like Na, Co, Cu, Fe, Cs, Hg, Pr, Cr, Fe, Ti elements in addition to Co^{+1}, Cu^{+1}, Cs^{+1}, Fe^{+1}, Ba^{+2}, Cr^{+1}, Mg^{+2}, and Mn^{+1} ions.

From samples irradiated by 30, and 60 mJ, heavy metals (Fe, Hg, Cr, Ti, Mn, Mg) concentrations were calculated using the calibration method.

At 30mj, (Fe, Hg, Cr, Ti, Mn) had different concentrations, Cr, Hg, and Ti were appeared with high concentration in the five samples. In sample (3) Ti had the highest concentration. Also at 60 mJ, (Fe, Cr, Ti, Mg) were appeared with low concentrations compared with the concentrations of the same concentration at 30 mJ. This thesis is benefit in controlling the pollution at industrial water [22].

M.A. Gondal, , Y.B. Habibullah, Umair Baig, L.E. Oloore in May 2016 used 266 nm UV pulsed-LIBS in direct spectral analysis of tea samples (six brands of tea in the wavelength range of 200–900 nm). The major toxic elements detected in tea samples were bromine and chromium. Nutritional elements detected in tea samples were iron, calcium, potassium and silicon. The plasma parameters (electron temperature and electron density) were also determined. The concentration of iron, chromium, potassium, bromine, copper, silicon and calcium detected in all tea samples was between 378–656, 96–124, 1421–6785, 99–1476, 17–36, 2–11 and 92–130 mg L−1 respectively. The limits of detection estimated for Fe, Cr, K, Br, Cu, Si, Ca in tea samples were 22, 12, 14, 11, 6, 1 and 12 mg L−1 respectively. Results with LIBS system are in good agreement with ICP-MS results [23].

In 2016 C.M. Ahamera, , ,S. Eschlböck-Fuchsa, , P.J. Kolmhofera, R. Rösslerb, N. Hubera, J.D. Pedarniga, used LIBS of major and minor oxides in steel slags: Influence of detection geometry and signal normalization.

Slag from secondary metallurgy in industrial steel production is analyzed by (LIBS). The major oxides CaO, Al2O3, MgO, SiO2, FeO, MnO, and TiO2 are determined by calibration-free LIBS (CF-LIBS) method. For the minor oxide P2O5 calibration curves are established and the limit of detection (LOD) was determined. The optical emission of the laser-induced plasma is measured for

different detection geometries and varying sample position relative to the focal plane of the laser beam. LIBS spectra, plasma parameters, and analytical results are very similar for light collection with optical fibers close to the plasma ("direct detection") and at remote position ("collinear detection"). With collinear detection, the CF-LIBS calculated oxide concentrations are insensitive to sample position along the optical axis over wide range. The detection limits and the prediction errors of minor P_2O_5 depend on the major slag element used for signal normalization. With Mg and Si as internal reference elements the LOD values are 0.31 wt% and 0.07 wt%, respectively. The RMSEP values are lowest for signal normalization to Si. Calculations of the optical emission of ideal plasma support the experimental preference for Si as reference element in the phosphorous calibration [24].

In 2016 Hervé K. Sanghapia, Jinesh Jainb, , Alexander Bol'shakovc, Christina Lopanob, Dustin McIntyred, Richard Russoc used LIBS for the Determination of elemental composition of shale rocks from the Marcellus.

Powdered samples were pressed to form pellets and used for LIBS analysis. The matrix effect is substantially reduced using the partial least squares calibration method. Predicted results with LIBS are compared to ICP-OES results for Si, Al, Ti, Mg, and Ca. As for C, its results are compared to those obtained by a carbon analyzer. The limits of detection (LODs) obtained for Si, Al, Ti, Mg and Ca are 60.9, 33.0, 15.6, 4.2 and 0.03 ppm, respectively. An LOD of 0.4 wt.% was obtained for carbon. This study shows that the LIBS method can provide a rapid analysis of shale samples and can potentially benefit depleted gas shale carbon storage research [25].

T Zhang, D Xia, H Tang, X Yang, H L in 2016 used LIBS integrated with random forest (RF) for the identification and discrimination of nine steel grades. The classification and recognition of the steel grade was completed by

investigating their physical and chemical properties. Two parameters of the RF were optimized by out-of-bag (OOB) estimation. The generation ability of RF model was evaluated by OOB estimation and 5-fold cross-validation (CV). Compared with the partial least squares discriminant analysis (PLS-DA) and support vector machines (SVM), the classification of steel samples based on RF model shows a better predictive performance. It has been confirmed that RF method is promising for automatic real-time, fast, reliable, and robust measurements; and the system can be integrated into portable form for non-specialist users [26].

In 2017 Jinmei Wang,Shuwen Xue,Peichao Zheng,Yanying Chen &Rui Peng used LIBS for determination of Lead and Copper in Li gusticum wallichii. The laser energy and delay time were optimized to obtain best spectral quality. The limits of detection for lead and copper were 15.7 and 6.3 µg g−1, respectively. Multiple linear regression models between the laser-induced breakdown spectroscopy intensity and the mass fraction of lead and copper were constructed. Good agreement was observed between the actual concentrations and predicted values obtained by the models. These results demonstrate that the laser-induced breakdown spectroscopy coupled with multiple linear regressions is suitable for the determination of heavy metals in Chinese traditional medicine [27].

 M. M. Nasr, M. A. Gondal, M. M. Ahmed, M. M. Yousif and N. A.Al-Muslet in 2018 used laser induced breakdown spectroscopy in direct spectral analysis of different gum Arabic samples: Nd:YAG laser beam at 266 nm, a pulse width of 8ns, a frequency of 20 Hz and 40 mJ was focused on GA samples and detected high concentrations of calcium, potassium, magnesium, zinc, iron, carbon, copper and fluorine present in these GA samples. The concentration of each element varies from one sample to another. The resultant spectrum was

collected in the range 270-720 nm which has most of the neutral and singly ionized atomic spectral lines [28].

Aissa Harhira, Josette El Haddad, Alain Blouin, and Mohamad Sabsabi in 2018 Used Laser-Induced Breakdown Spectroscopy to determination of Bitumen Content in Athabasca (Canada) Oil Sands: Evaluation of bitumen content in oil sands feedstock is important to control the extraction process and improve the recovery efficiency. Current standard techniques for bitumen determination in oil sands ore suffer whether from their time-consuming labor intensive method of sample preparations or from requiring a high number of samples for calibration purposes. The analysis of bitumen ore samples is very challenging for the analytical chemist due to its nature of several phases of wet and dry particles and heterogeneous mixture of clay, bitumen, water, and solid contents. LIBS is used to determine rapidly and without sample preparation the bitumen content in oil sands ores. A qualitative study by principal component analysis was first done, and then a partial least-squares method was performed to assess the feasibility of determining bitumen by LIBS. The results show a good correlation between LIBS spectra and bitumen content and a prediction averaged absolute error around 0.7%. This method demonstrates that the LIBS is a promising tool for rapidly assessing oil sands ore grades either in the lab, at-line, or online. Elemental composition of solids is also investigated [29].

G.S.SenesiaD.ManzinibO.De Pascalea in 2018 used LIBS to the diagnostic analysis of stone monuments the development of portable handheld instruments able to perform non-invasive, spatially resolved, multi-element, *in-situ* analysis has provided an impressive impulse to the scientific investigation of cultural heritage materials. In this work, the design of a handheld LIBS instrument and the first test measurements performed on a fragment of a sedimentary rock monument are presented. A full broadband LIBS emission spectrum with a point and shoot operation was recorded directly within few seconds, so

providing information on the elements present in the weathered layer in comparison to the stone surface. Further, the Calibration Free (CF)-LIBS approach was used to test the possibility to obtain a suitable quantitative composition of the main elements present in the sample [30].

N. H. Thomas B. L. Ehlmann D. E. Anderson S. M. Clegg O. Forni S. Schröder W. Rapin P.- Y. Meslin J. Lasue D. M. Delapp M. D. Dyar O. Gasnault R. C. Wiens S. Maurice in 2018 used LIBS for Characterization of Hydrogen in Basaltic Materials in application to MSL ChemCam Data.

The Mars Science Laboratory rover, Curiosity, is equipped with ChemCam, a laser- induced breakdown spectroscopy (LIBS) instrument, to determine the elemental composition of nearby targets quickly and remotely. We use a laboratory sample set including prepared mixtures of basalt with systematic variation in hydrated mineral content and compositionally well characterized, altered basaltic volcanic rocks to measure hydrogen by characterizing the H-alpha emission line in LIBS spectra under Martian environmental conditions. The H contents of all samples were independently measured using thermo-gravimetric analysis.

We found that H peak area increases with weight percent H for our laboratory mixtures with basaltic matrices. The increase is linear with weight percent H in the mixtures with structurally bound H up to about 1.25 wt.% H and then steepens for higher H- content samples, a nonlinear trend not previously reported but potentially important for characterizing high water content materials. To compensate for instrument, environmental, and target matrix-related effects on quantification of H content from the LIBS signal, we examined multiple normalization methods. The best performing methods utilize O 778- and C 248- nm emission lines. The methods return comparable results when applied to ChemCam data of H- bearing materials on Mars. The calibration and normalization methods tested here will aid in investigations of H

by LIBS on Mars with ChemCam and SuperCam. Further laboratory work will aid quantification across different physical matrices and heterogeneous textures because of differences we observed in H in pelletized and natural rock samples of the same composition [31].

Chapter Three
Materials and Methods

3.1 Introduction:

This chapter illustrates the used of promising technique (LIBS) to detect the elements in crude oil samples collected from three different locations in Sudan.

The growth of petroleum industry worldwide and marketing of petroleum products has resulted in the pollution of the environment with heavy metal due to oil spills and leakage from oil tanks or tanker trucks and waste oil dumps. The effects of such pollution on the environment, humans, live stocks, wild life, crops and soil have been enormous [32].

Crude oil according to its nature composed of many elements, the concentrations of each elements differs from location to another (appears as differ intensities) and from oilfield to other according to the location that take the sample for it.

Crude oil occurs underground, at various pressures depending on depth. It can contain considerable natural gas, kept in solution by the pressure. In addition, water often flows into an oil well along with liquid crude and gas. All these fluids are collected by surface equipment for separation.

Those elements form a large variety of complex molecular structures, some of which cannot be readily identified. Regardless of variations, however, almost all crude oil ranges from 82 to 87 percent carbon by weight and 12 to 15 % hydrogen by weight [8].

A type of fossil fuel, crude oil can be refined to produce usable products such as gasoline, diesel and various forms of petrochemicals.

The instrumentation of LIBS is relatively simple as compared to other analytical techniques such as mass spectrometry, laser-induced fluorescence, inductively coupled plasma-atomic emission spectrometry (ICP-AES) etc.

In this work LIBS technique was used to detection of basic elements in crude oil sample collecting from three different oilfields in Sudan. The irradiation of the sample was done by using Q-Switched ND-YAG Laser 1064 nm set with pulse energy 150, 170, 190 mJ. Such plasma emission spectrum was collected using wide band fused-silica optical fiber of one-meter length connected to a portable Ocean Optics USB 2000+ spectrometer of range (200 nm to 1100 nm).

3.2 **Samples collection:**

Three crude oil samples collected from different oilfields in Sudan were used in this work. The first one is Rawat field, located in bloc "25" in the state of White Nile, closed to the common border with South Sudan.

The second one is new oilfield at Hadida on the border between East Darfur and South Kordofan.

The last one is Melut Basin is a rift basin in South Sudan. It is situated in the states of Upper Nile and Jonglei, south of the capital Khartoum and east of the river Nile. The export pipeline is also known as the PetroDar Pipeline after the name of the consortium which operates it. Crude oil from the Melut Basin is known as "Dar Blend"[1in ch3,4].

3.3 The experimental setup:

The experimental setup in this thesis was arranged as shown in Fig (3.1)

Fig (3.1): experimental setup

Chemical structure of crude oil:

The hydrocarbon chains of Al-naphthenic paraffin and aromatic compounds are included in the basic installation of petroleum 80-90% g. There are a relatively tiny amount of oxygenic compounds, sulfur, and nitrogen.
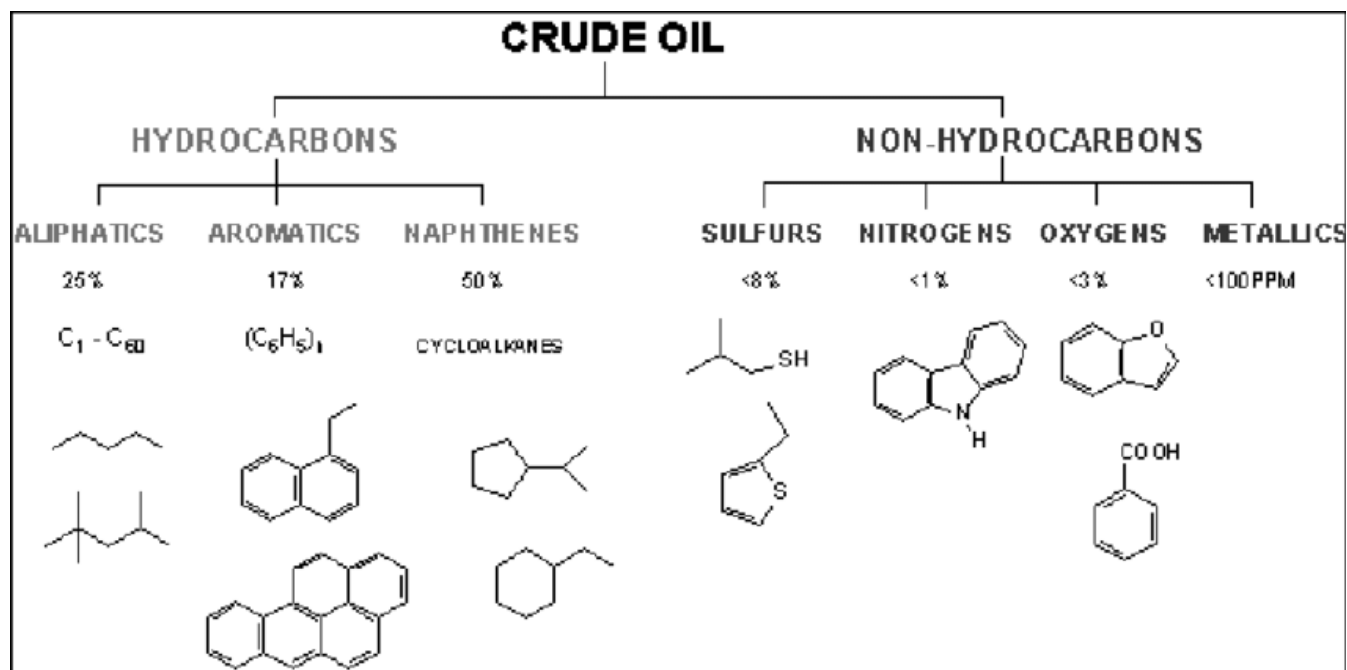
Fig (3.2) Chemical structure of crude oil [33]
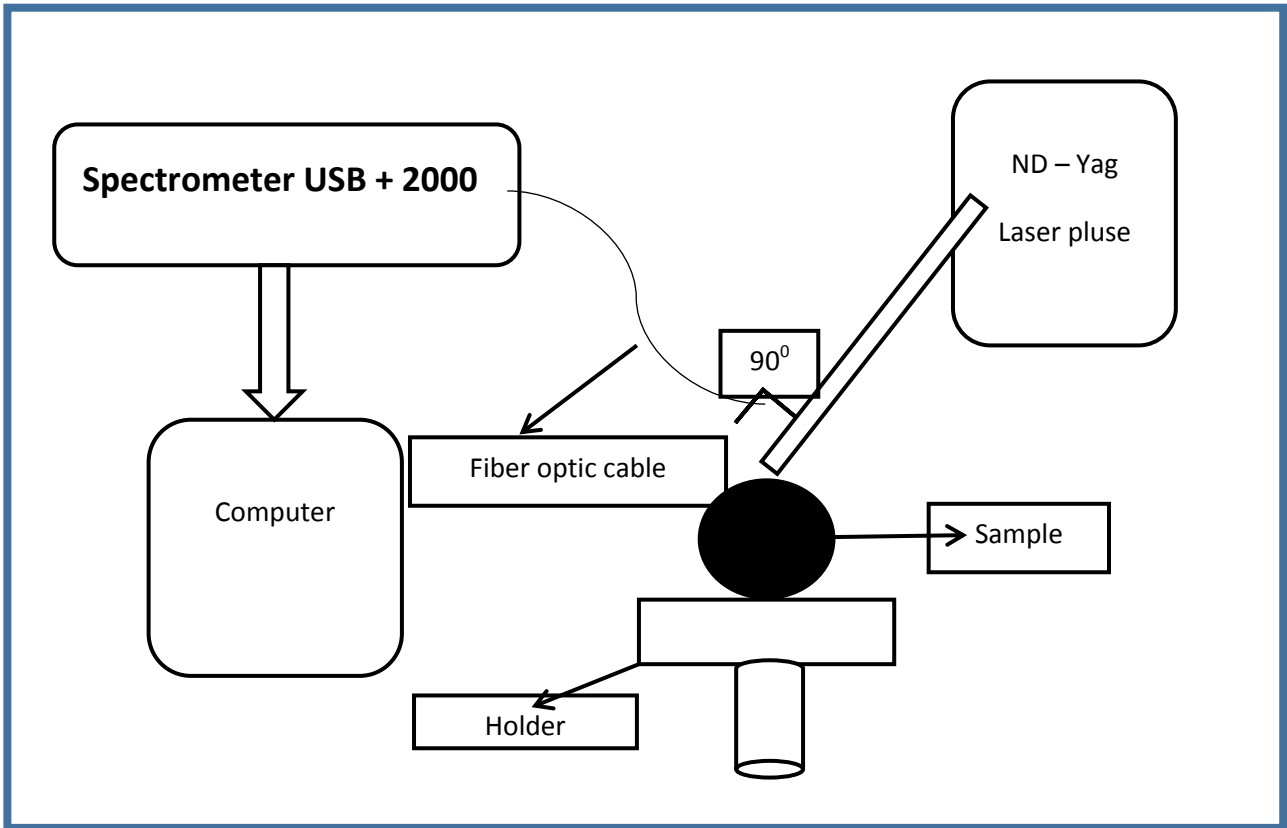
Figure (3.3): Schematic diagram of LIBS setup

3.3.1 Nd-YAG LASER:

Q-switched Nd – YAG Laser System structure is mainly consisted of the following units: Power Supply, Laser Hand piece, Control Unit and Cooling System. The specifications of the Nd – YAG laser was shown in table (3.1).

Table (3.1): laser specifications:

component	Specifications
Company	Shanghai Apolo Medical Technology Co., Ltd China
Power Supply:	~230V, 50/60Hz
Model	HS-220
Laser Type	Q switched Nd - YAG Laser
Laser wavelength：	1064nm & 532nm
Weight	20 kg
Pulse width：	10ns
Repeat frequency	1, 2, 3, 4, 5 HZ
Lead light method	directly export laser
The light spot diameter	2~8mm
Power supply	90-130V, 50Hz/60Hz or 200-260v, 50Hz
Environment temperature	5˚C～40˚C
Relative humidity：	80%
Cooling system	the water-cooling + the air cooling inside. System device overview
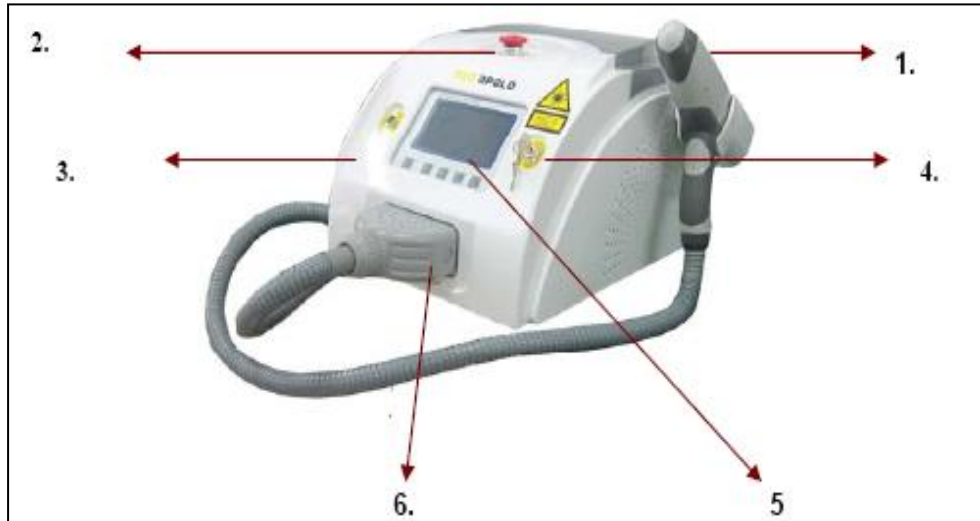
Fig (3.4): Q-switched Nd-YAG laser

Front view of Nd:YAG laser is shown in fig (3.4):

1 .Laser hand piece

2. Emergency switch

3. Main host

4. Key switch

5. LCD control panel

6. Hand piece Connector.

The temperature display and protection:

The system has the temperature display function, which can monitor the temperature of the circulating water, when the temperature of the circulation water exceed prescriptive protection Temperature," the water temperature lead high" will show on the screen, at the same time the Buzzer gives an alarm and the instrument won't continue to work. When the temperature of Circular water declines under the protect temperature the instrument can work normally [34].

3.3.2 Glass cell:

The galas cell used to put the samples inside it.

3.3.3 Detection System:

The detection system was consists of:

Spectrometer:

The diagram of a simple spectrometer is shown in fig (3.6). Light enters the spectrometer via the entrance slit and then passes through several parts: an objective lens, a grating, and an exit slit. This combination of parts functions as a mono-chromator, a device that selects only one color (actually, a narrow band of wavelengths) from all of the wavelengths present in the source. A particular wavelength is selected, using the wavelength control, by adjusting the angle of the grating. This works because different wavelengths of light reflect off the grating at different angles. The net result is the separation of white light into a "rainbow," much like the effect of light transmitted through a prism of glass. The selected wavelength is at the center of the narrow band of wavelengths passing through the slit. The light then strikes a detector that generates a voltage in proportion to the intensity of the light hitting it. That voltage is then used to drive a read-out device that is designed to provide data in a format such as intensity [2].
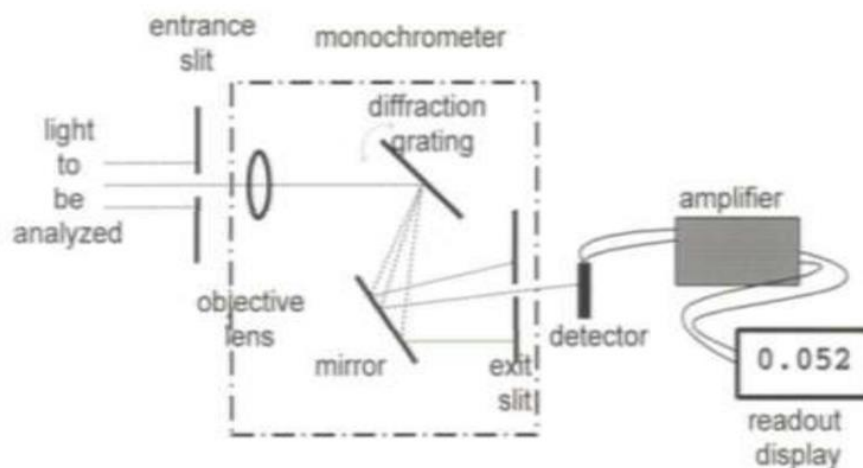
Figure (3.5): Diagram of a simple spectrometer [2]

The spectrometer: The spectrometer used in this work was Ocean Optics LIBS USB +2000 of spectral range from 200 nm t0 1100 nm range.

Fig (3.6): Ocean Optics USB +2000 [35]

Table (3.2): spectrometer specifications [35]

PHYSICAL	
Dimensions:	89.1 mm x 63.3 mm x 34.4 mm
Weight:	190 g
DETECTOR	
Detector:	Sony ILX511B (2048-element linear silicon CCD array)
Detector range:	(200-1100) nm
Pixels	2048 pixels
Pixel size:	14 μm x 200 μm
SPECTROSCOPIC	
Optical resolution:	~0.1-10.0 nm FWHM (configuration dependent)
Signal-to-noise ratio:	250:1 (full signal)
A/D resolution:	16 bit
Dark noise:	50 RMS counts
Dynamic range:	8.5 x 10^7 (system); 1300:1 for a single acquisition
Integration time:	1 ms – 65 seconds
Stray light:	<0.05% at 600 nm; <0.10% at 435 nm
Corrected linearity:	>99%
ELECTRONICS	
Power consumption:	250 mA @ 5 VDC

Inputs/Outputs:	Yes. Onboard digital user programmable GPIOS
Trigger modes:	4 modes
Stobe functions:	Yes
Gated delay feature:	Yes
Connector:	22-pin connector

3.4 Methodology:

Q-switched Nd: YAG laser was used to irradiate the samples and produce its plasma. The emission spectra of the plasma were collected via optical fiber and analyzed by USB +2000 spectrometer of spectral range 200nm to 1100nm. The USB2000 interfaces to computer with Windows operating system.

A laser pulse with 120mJ energy was focused on the glass plate without the sample and the spectrum was recorded and saved as dark spectrum .The sample was then irradiated with the same energy and the spectrum of the emitted plasma was recorded. The net spectrum was obtained by subtracting the dark spectrum. This step was repeated for energy pulse 150, 170, 190 mJ for all the three samples.

The resulted emission spectrum was analyzed using Atomic Spectral Database where the elements in the sample were identified.

Chapter four

Results and Discussion

4.1 Introduction:

This chapter discusses data of three different samples of crude oil collection from three different oilfields in Sudan.

The LIBS emission spectra are recorded at a 90˚ angle to the direction of incident laser pulse. Software built in the spectrometer reads the data from the chip and reconstructs the spectrum. This makes it possible to measure a long wavelength range.

In this study, and for the optimization of various parameters of LIBS, the different stoichiometric samples of C, H, O, N, S (main component), also Fe, Cu, Ni and V were detected in crude oil samples. The spectra of the standard samples were recorded.

4.2 The qualitative results:

Figures show the LIBS emission spectra for three Crude Oil samples Hadida, Rawat and Melut oilfields irradiated by Pulse Energy (120, 150 170 and 190) mJ.

4.2.1 Hadida oilfield irradiated by 120 mJ:
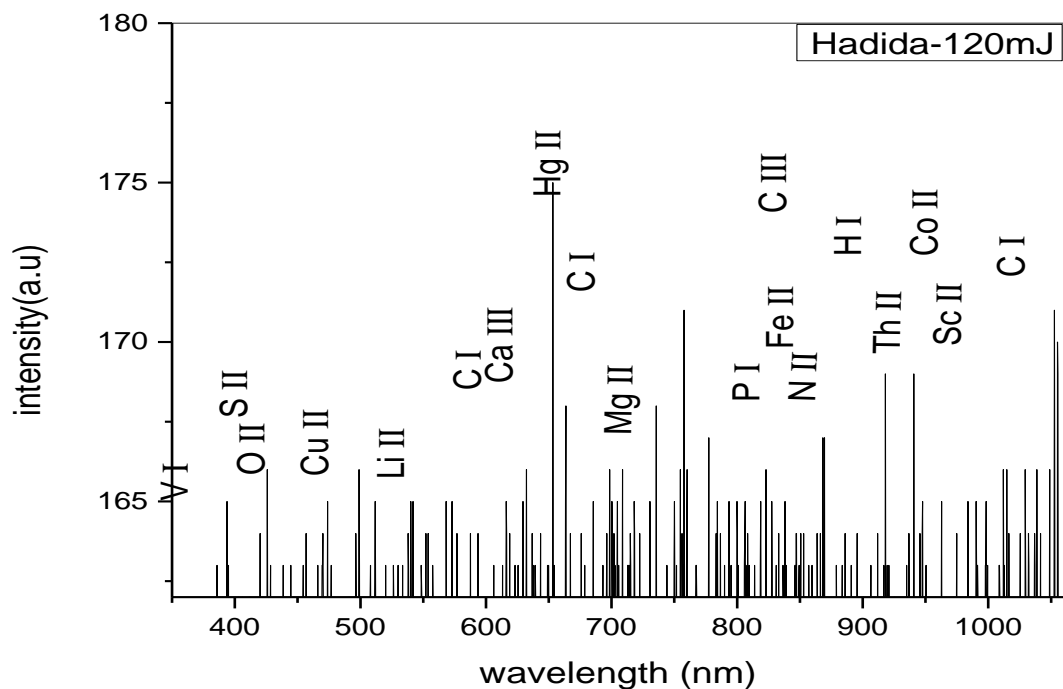
Fig (4.1): LIBS emission spectrum of Hadida oilfield irradiated with

120mJ pulse energy

Table (4.1): Data of Hadida oilfield after irradiated by 120 mJ:-

λ(nm)	Intensity (a.u)	Element
385.48	163.075697	V I
393.94	165.073421	S II
428.13	163.039841	O II
439.19	163.08082	Mn II
457.10	164.03358	Be III
465.90	163.039841	Cl I
466.70	163.085942	Fe III
470.94	163.516221	N II
476.30	163.06033	Sc I
495.67	163.982356	Ar I
496.98	163.992601	Cu II
498.95	165.990324	V I

λ(nm)	Intensity (a.u)	Element
499.74	164.463859	Ne I
508.05	163.039841	Tm I
512.11	165.063176	Fe II
520.42	163.101309	N IV
541.91	165.052931	O II
'541.09	164.33067	Li II
547.93	163.085942	S II
551.66	164.059192	Ar II
547.93	163.06033	S II
554.34	164.079681	N II
594.01	164.054069	C I
606.20	163.055208	C I
612.22	163.034718	W I
617.43	165.073421	Cu II
618.89	164.07968	V V
623.12	163.075697	Fe I
647.87	163.009106	S IV
625.10	175.062038	Hg II
654.22	171.86568	Ca III
722.91	164.084804	O II
754.48	166.077405	Sc I
755.95	164.054069	Fe I
777.10	164.12066	Sc I
795.81	163.08082	V I
817.96	164.079681	Fe II
831.64	163.085942	Hg I
835.87	163.08082	C III
849.69	163.06033	Fe I
850.22	162.97325	H I
865.50	164.12583	S V
867.60	164.525327	N II
869.88	167.404098	V II
878.50	163.06033	B I
1051.34	171.035857	N I

λ(nm)	Intensity (a.u)	Element
1053.15	171.051224	V I
1054.00	171.046101	Ba I
1054.80	170.139442	C I
1055.28	170.118953	Fe II
1055.60	169.104724	Si III
1056.75	169.104724	Si III

4.2.2 Irradiation of Hadida with 150 mJ:
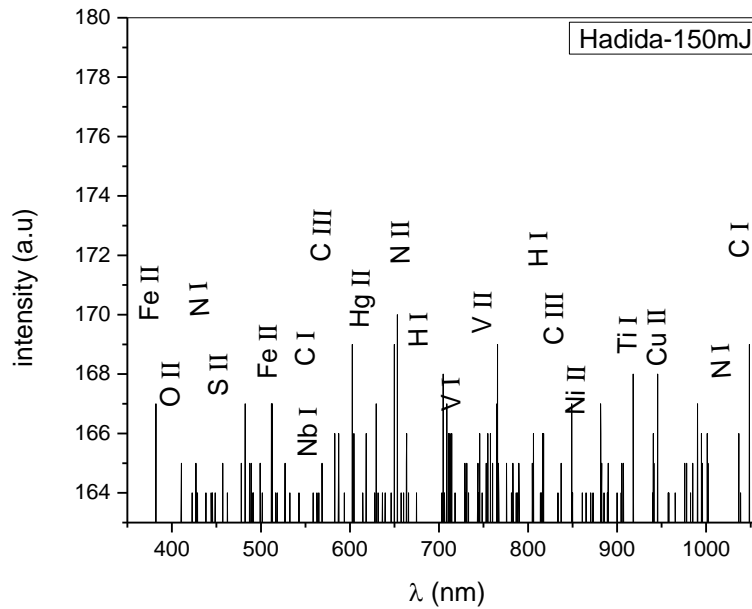
Fig (4.2): LIBS emission spectrum of Hadida oilfield irradiated with 150mJ pulse energy

Table (4.2): The data of Hadida oilfield after irradiation by 150 mJ:

λ(nm)	Intensity (a.u)	Element
381.41	167.044394	Fe II
382.71	167.044394	Mo I
427.15	165.094764	V I
428.13	164.064314	O II
444.24	164.059476	N I
446.35	164.059476	S II
477.45	165.065737	V I
488.03	165.065737	Hg II
490.14	164.078828	Cu II
500.72	164.015936	Er I
499.74	165.060899	Ne I
511.79	167.039556	Mn I
512.11	167.044394	FE II
517.65	1645.103017	Ni I
532.79	164.064314	Cu II
559.48	163.972396	Xe II
563.71	163.972396	Cu II
564.53	164.035287	Fe II
568.77	165.041548	V I
581.77	166.042971	N III
593.5	164.103017	Kr III
587.15	165.549516	Hg II
603.1	169.052077	V II
604.39	166.042971	Cs III
614.17	164.083665	Hg II
618.4	166.096187	Ne III
632.08	164.020774	Sc II
638.26	164.20774	Ar II
649.98	169.071429	Ti III
652.11	170.014798	Hg II
654.22	167.310472	Ca III
656.29	163.991747	H I
657.47	163.996585	Nb I

λ(nm)	Intensity (a.u)	Element
659.58	163.996585	N I
661.05	163.991747	N III
665.1	164.015936	C I
674.88	164.059476	Fe II
706.29	164.015936	Ni I
713.29	165.307627	Fe I
731.19	165.060899	V I
744.87	164.514229	Nd II
749.1	164.011098	Eu I
754.53	166.028458	N II
756.62	166.028458	Fe II
757.25	166.018782	Fe II
755.14	166.018782	O III
759.53	165.060899	C III
757.9	165.989755	Cu II
767.02	165.03671	V II
780.84	164.069152	Nd II
782.96	165.012521	Mo I
782.05	163.972396	Cu II
782.15	163.299943	Sc I
787.69	164.035287	Fe II
788.99	165.046386	Ni III
815.34	164.088503	S I
817.96	166.018782	Fe II
833.09	164.001423	H I
837.44	165.0700575	H I
850.03	167.083096	C III
860.43	164.064314	N II
864.84	164.064314	S I
872.32	164.064314	Co II
882.89	165.070575	Al I
889.6	165.070575	Ni II

λ(nm)	Intensity (a.u)	Element
918.28	168.065168	Cr II
946.06	168.55492	N I
956.56	164.093341	Cu II
964.84	164.064314	O II
976.33	165.089926	Fe II
983.16	164.001423	Th I
989.51	167.083096	Fe II
995.87	165.070575	Cr II
1001.08	166.028458	O II
1002.21	165.070575	Fe II
1002.37	165.046386	Xe I
1036.56	166.042971	N I
1038.21	164.03045	C I
1047.95	169.032726	Th I
1053.95	167.073421	N I
1054.8	171.103301	C I

4.2.3 Irradiation of Hadida with 170 mJ:
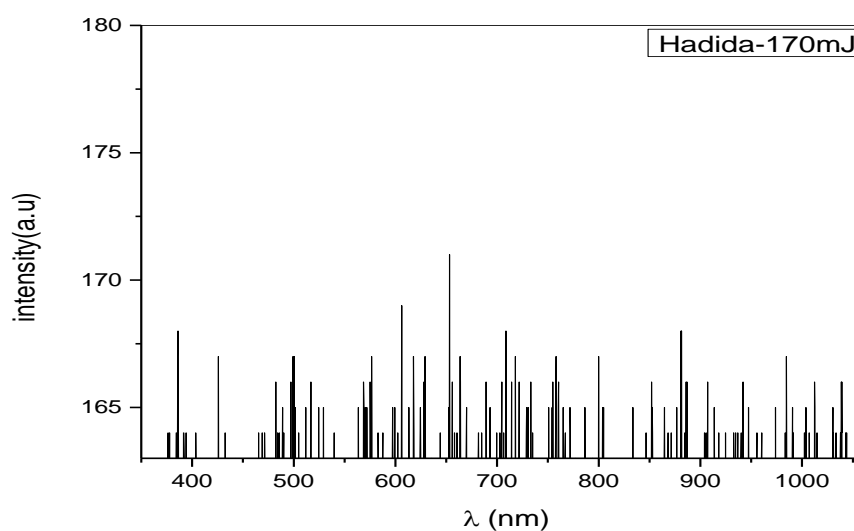
Fig (4.3): LIBS emission spectrum of Hadida irradiated with 170mJ pulse energy

Table (4.3): The data of Hadida oilfield after irradiation by 170 mJ:-

λ(nm)	Intensity (a.u)	Element
377.18	164.015936	Nb I
385.64	168.04079	Fe I
385.48	168.070006	Sc II
391.33	164.064314	Hg II
425.21	167.083096	C III
465.40	164.083665	Cl I
469.63	164.06314	O II
470.94	164.064314	N II
485.26	164.040125	Ni II
486.07	164.040125	H I
486.12	165.065737	H I
490.14	164.122368	Cu II
500.56	165.128628	V I
505.28	164.040125	Ti I
516.35	166.052647	Ne I
539.13	164.103017	Hf II
568.61	166.06716	Fe I
570.72	165.060899	Si III
587.96	164.098179	S I
601.63	163.566022	C I
612.22	165.152817	Ca I
623.78	164.325555	Zn I
627.20	166.02362	Sr I
644.12	164.112692	Cu II
654.70	166.81218	N V
655.36	166.105862	Li II
656.27	164.044963	H I
661.05	163.977234	N I
663.16	167.09761	Br I
669.35	164.359419	Sm II
670.50	165.08025	V I
682.03	164.044963	Ho I

λ(nm)	Intensity (a.u)	Element
684.82	164.054639	S II
689.95	166.06716	Ga II
700.09	164.054639	N II
702.22	164.035287	C I
706.29	164.098179	Ni I
704.34	166.047809	Sc II
709.05	168.089357	Ar II
715.25	166.018782	Co III
718.83	165.583381	Cs II
717.37	167.063745	Mn II
721.60	166.06718	C I
728.43	165.022197	Cd II
729.39	165.031873	Cr I
755.14	166.0623	O III
754.53	166.062322	N II
757.25	166.521912	Fe II
833.09	165.075413	V II
846.80	164.78828	V I
852.30	166.062322	Th I
865.00	165.056061	Na VII
867.12	163.54667	Al II
877.69	165.056061	3He I
885.51	166.038133	S IV
904.54	164.025612	Xe I
906.72	164.03045	Hg I
932.22	164.040125	Fe II
955.33	164.054639	3He I
959.91	164.035287	Cs III
973.58	165.060899	Cu II
984.15	167.058907	Fe II
990.01	165.007684	Sc II
1014.72	164.040125	N I

λ(nm)	Intensity (a.u)	Element
1029.6	165.046386	S VI
1040.13	166.052647	Th I
1044.40	163.977234	V I
1052.00	169.056915	Li II
1054.80	170.077689	C I

4.2.4 Irradiation of Hadida with 190 mJ:
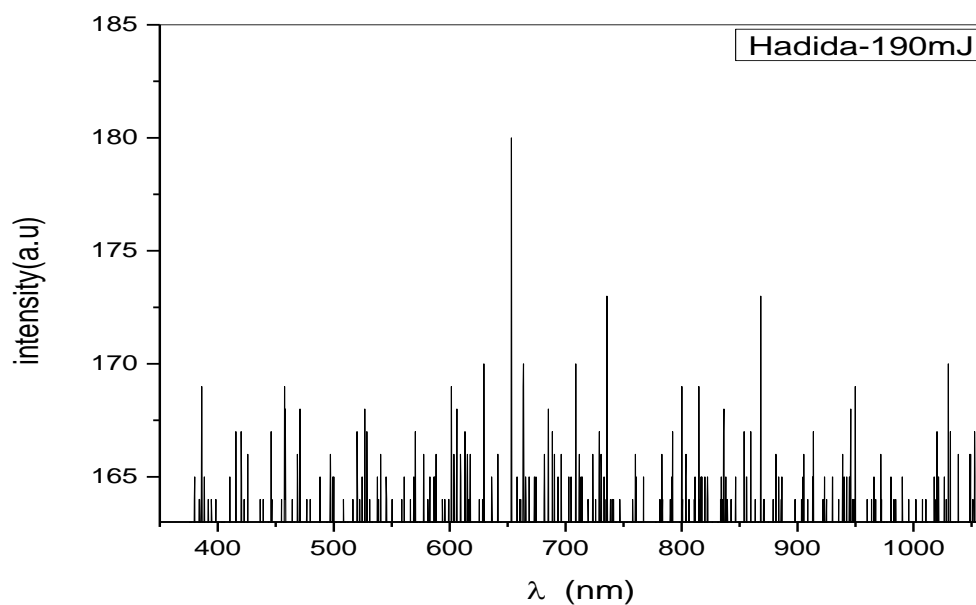
Fig (4.4): LIBS emission spectrum of Hadida oilfield irradiated with 190mJ pulse energy

Table (4.4): The data of Hadida oilfield after irradiation by 190 mJ:-

λ(nm)	Intensity (a.u)	Element
379.79	164.02675	H I
383.53	164.133182	H I
385.48	165.109846	V I
387.61	165.141434	C II
388.90	165.109846	H I
397.00	164.02675	H I
410.88	165.063745	O II
446.03	167.13745	Mn I
496.98	166.067729	Cu II
499.10	165.057769	Fe II
525. 96	165.057769	C I
526.60	165.834661	Fe II
528.72	167.077689	Ne VI
538.00	164.932271	Na VII
54. 98	165.111554	S I
545. 32	165.109846	Ni I
568.76	156.033865	V I
568. 62	167.02988	N II
576. 91	166.01992	O IV
578.53	165.398406	Mg I
577.39	166.037849	Si XIII
585.85	165.027888	Cu II
587.97	166.115538	S I
601.64	169.085657	C I
603.11	166.01992	V II
608.99	166.155378	Na VI
610. 08	166.109562	Cu III
615.80	166.109562	O I
629. 15	170.089641	Si III
652.26	180.063745	H I
668. 18	164.139442	S II
672.93	165.003984	N I

λ(nm)	Intensity (a.u)	Element
675.05	165.003984	C II
687. 74	167.10757	Th I
690.03	166.09761	N I
696.37	166.01992	S IV
702. 55	165.087649	O I
704. 68	165.087649	Nb I
713.30	165.087649	Fe I
713.95	166.103586	Cs II
722.42	166.025896	C I
728. 43	167.035857	Cd II
730.88	166.025896	Al II
783.78	166.047809	O IV
802.82	165.081673	C I
810. 97	165.111554	Fe II
814.71	169.079681	Sc I
821.38	165.081679	Ti I
816.50	16.057769	Nd I
835.00	168.069721	H I
837. 44	168.069721	H I
838.63	165.111554	N III
853.45	167.053785	O IV
856.54	165.069721	Ar II
867.12	170.119522	Al II
881.28	166.073705	V I
883.40	165.063745	Fe II
886. 28	165.057769	H I
922.79	165.11753	He I
939. 38	166.09761	Cl I
944. 61	165.087649	V II
946.06	168.039841	N I
950. 13	169.049801	Fe II

λ(nm)	Intensity (a.u)	Element
965.11	165.00996	Cu II
967.22	165.00996	S I
979.92	165.087649	Co II
990.49	165.00996	Th I
1018.00	165.00996	198Hg I
1022.25	165.087649	S IV
1020.28	167.131474	C I
1030.05	170.053785	Te I
1038.51	166.151394	Al II
1049.09	166.073705	Fe II
1055.44	165.087649	C I

LIBS has been used for compositional mapping, i.e., spatial mapping of the elemental composition of a sample, for a number of elements including (Fe, Cu .Li, He and so on) . Analysis of generating distribution maps of elements in Crude Oil sample collected from Hadida oilfield   were selected for the LIBS analysis by Pulse Energy (120, 150 170 and 190) mJ , number of mapping element increase when energy pulse increase   as show in table (1) ,table (2) , table (3) and table (4).

Sample (2) RAWAT OILFIELD:

4.2.5 Irradiation of Rawat with 120 mJ:
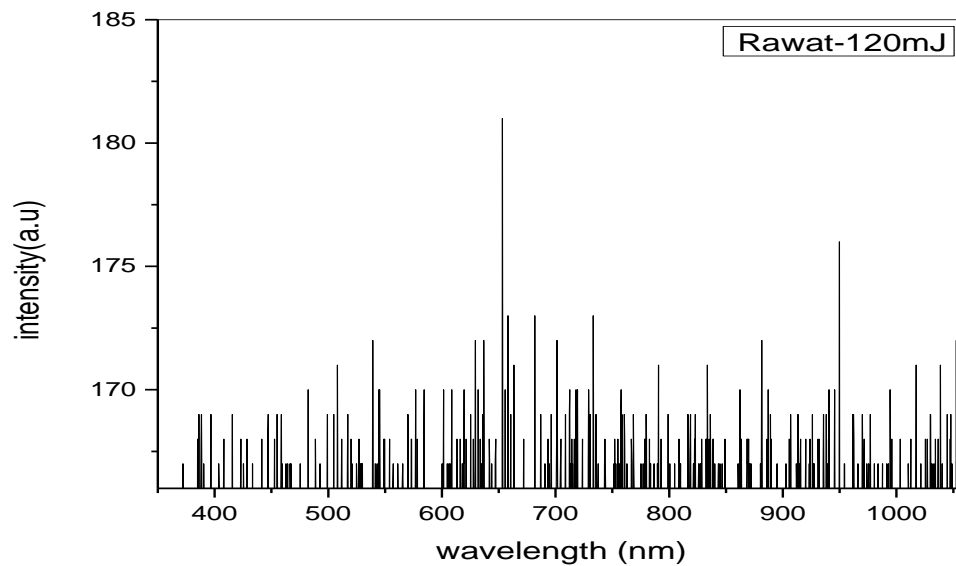
Fig (4.5): LIBS emission spectrum of Rawet oilfield irradiated with 120mJ pulse energy

Table (4.5): The data of Rawat oilfield after irradiation by 120 mJ:-

λ(nm)	Intensity (a.u)	Element
385.32	169.064314	W I
396.55	169.074559	Fe I
407.13	168.06033	Th I
415.75	169.059192	O IV
422.76	168.08082	Th II
428.13	167.993739	O II
441.96	168.126921	Pr II
446.19	168.20102	Fe I
447.5	169.054069	Kr II

λ(nm)	Intensity (a.u)	Element
445.38	168.188389	Ti I
446.02	168.25498	V I
452.38	168.25498	Sc I
481.18	170.022197	Sr I
499.43	169.084804	N II
504.95	169.089926	Ba III
545.32	170.109277	Ni I
577.23	170.041548	K I
608.97	608.966071	Hg II
619.19	170.085088	Cs I
625.57	169.078828	Ho I
652.26	181.062038	C II
663.82	171.047809	Ar I
660.89	169.035287	Cr I
696.71	169.044963	Na II
700.92	172.126636	Hg I
702.22	702.232921	C I
719.02	170.044394	O III
732.65	173.040979	N V
757.25	170.104439	Fe II
758.47	169.054639	Mg I
767.83	169.098179	Sc IV
835.87	169.020794	C III
887.33	170.060899	C I
886.79	170.03671	Fe II
889.39	169.054639	Co II
925.39	169.103017	Hg I
936.01	169.040125	Na II
937.82	169.044963	N IV
946.06	176.074274	N I
950.31	176.03671	Mg I
968.85	169.059476	O III
970.1	168.619237	S II
994.13	170.041548	C I

λ(nm)	Intensity (a.u)	Element
1017.35	170.984917	Fe II
1088.51	171.0478	Al II
1044.99	169.02774	C I
1047.96	169.088503	K I
1052.21	172.044394	V I

4.2.6 Irradiation of Rawat with 150 mJ:
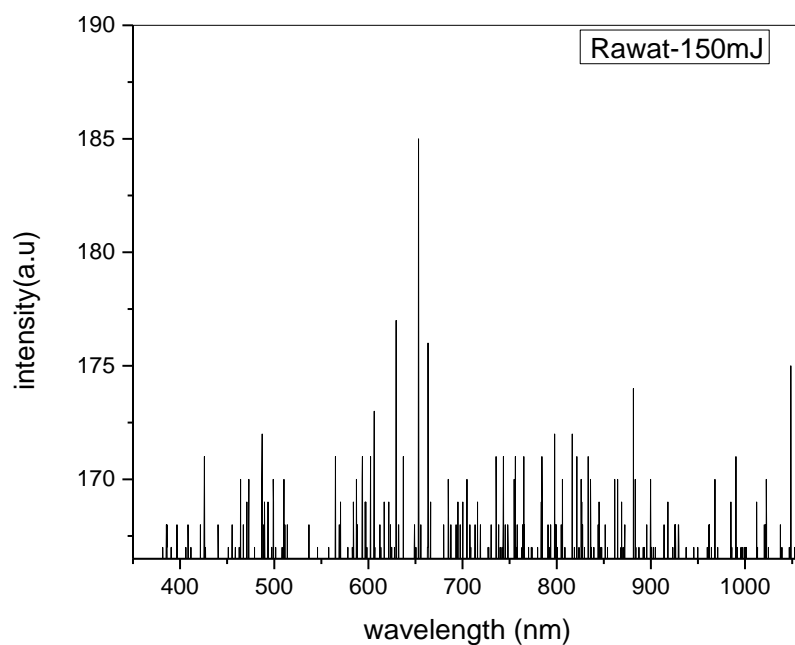
Fig (4.6): LIBS emission spectrum of Rawet oilfield irradiated with 150mJ pulse energy

Table (4.6): The data of Rawat oilfield after irradiation by 150 mJ:-

λ(nm)	Intensity (a.u)	Element
381.41	167.092772	Fe II
385.48	168.069437	V I
391.18	167.031303	O III
384.83	168.124075	Nd II
421.30	168.103586	C I
425.53	17103358	C III
440.66	168.076266	V I
451.24	167.099602	Th I
462.99	170.097894	Xe II
472.39	169.565168	Hg I
479.07	167.065452	Ne I
498.44	170.077405	Fe II
509.67	168.417758	Sc I
513.90	168.062607	Fe II
564.53	171.081389	Nb I
584.87	166.587365	Fe III
585.85	168.861696	Cu II
593.50	171.095048	Cr I
595.61	169.052931	W I
697.02	167.072282	C I
603.10	169.339784	V II
605.26	173.068867	S I
601.64	171.02675	C I
611.58	166.689812	C I
616.95	169.052931	Fe
623.76	168.042117	N I

λ(nm)	Intensity (a.u)	Element
6.7.78	171.122368	Cu II
650.46	167.126921	N II
665.93	169.08025	C I
687.08	168.192373	V I
692.62	168.076266	Ti I
705.31	170.029596	V I
707.43	168.076266	W I
715.90	169.052931	O IV
716.06	169.025612	Co III
718.83	168.048947	Cs II
727.29	167.072282	Ar I
731.55	168.048947	V I
726.97	167.003984	Mn II
736.53	168.363119	O III
740.16	166.573705	Fe I
743.58	171.074559	V I
756.12	171.122368	Mn
783.61	169.04611	Al I
793.38	168.151394	Cl I
790.29	168.048947	Xe III
797.29	172.079112	Te I
798.59	168.636312	W I
804.95	170.082812	V I
807.05	168.125783	Si I
816.49	172.111838	Nd I
820.72	171.09078	Ti I
822.03	171.038418	Fe I
826.25	170.102447	Si III
835.87	170.07359	C III
844.33	168.14518	Hg I

λ(nm)	Intensity (a.u)	Element
851.80	168.027604	He I
872.80	168.04724	Si I
881.28	174.173591	V I
883.39	170.004269	Fe II
894.95	168.04724	Cr I
913.99	168.06033	Al I
918.21	168.996301	N IV
926.72	167.975242	C II
960.54	167.975242	Al III
962.67	167.975242	As I
989.36	171.012237	Fe II
1012.62	169.140296	N II
1021.08	168.034149	Ne I
1037.90	168.027604	Fe I
1048.41	175.004838	S II

4.2.7 Irradiation of Rawat with 170 mJ:
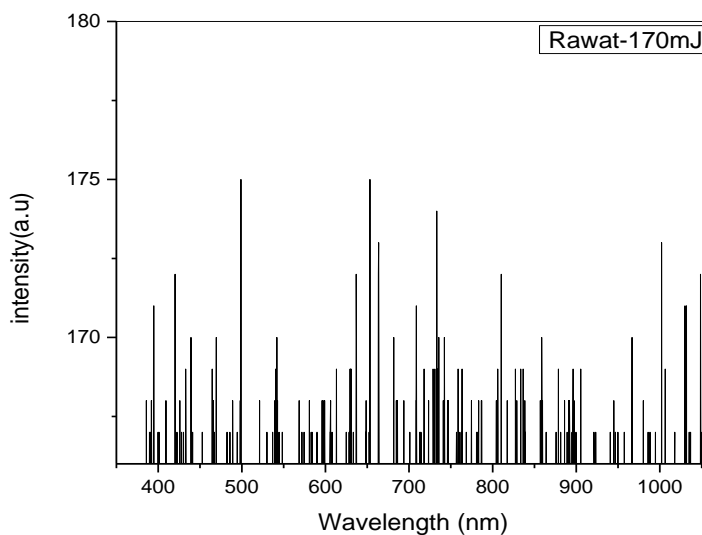
Fig (4.7): LIBS emission spectrum of Rawet oilfield irradiated with 170mJ pulse energy

Table (4.7): The data of Rawat oilfield after irradiation by 170 mJ:-

λ(nm)	Intensity (a.u)	Element
385.48	168.02519	V I
389.71	167.02632	Fe V
390.36	167.04937	Hg I
391.83	168.02519	Mn I
393.94	171.02177	S II
395.09	171.08324	Xe I
400.61	167.05706	Cu II
419.67	172.05137	O II
422.93	167.02632	C IV
424.87	168.02519	Ni II
431.71	169.04326	O II
439.20	170.02675	V I
463.61	169.07015	Ne I
486.56	167.04553	Ti II
521.88	168.02903	Fe II
536.70	167.03017	N I
543.68	167.05976	C I
486.12	167.08307	H I
547.93	167.05976	S II
548.25	167.01864	Cu II
612.87	169.03557	Mn II
652.26	175.05179	C II
654.37	172.036	O V
694.24	167.99445	W I
713.29	167.05322	Fe I
715.25	167.00327	Co III

λ(nm)	Intensity (a.u)	Element
718.81	167.79852	N II
723.06	168.04824	Cr I
727.32	169.01252	S II
740.33	168.03287	Hg I
747.64	168.04439	O I
767.83	167.02248	Sc IV
773.86	167.02248	Cu II
804.61	168.05976	Mg II
806.95	168.41705	V I
809.04	172.06289	Hg I
835.87	169.05478	C III
824.99	166.05706	H I
828.64	168.12023	H I
880.62	167.03785	Th I
891.20	168.03671	Ca II
892.35	168.02134	Al I
920.82	167.01864	Cr I
950.13	167.05322	Fe II
994.55	167.05322	Co II
1002.37	173.04254	Xe I
1017.20	166.99943	C I
1029.98	171.04482	Th I
1035.58	167.03785	Th II
1047.32	172.02832	Fe II

4.2.8 Irradiation of Rawat with 190 mJ:
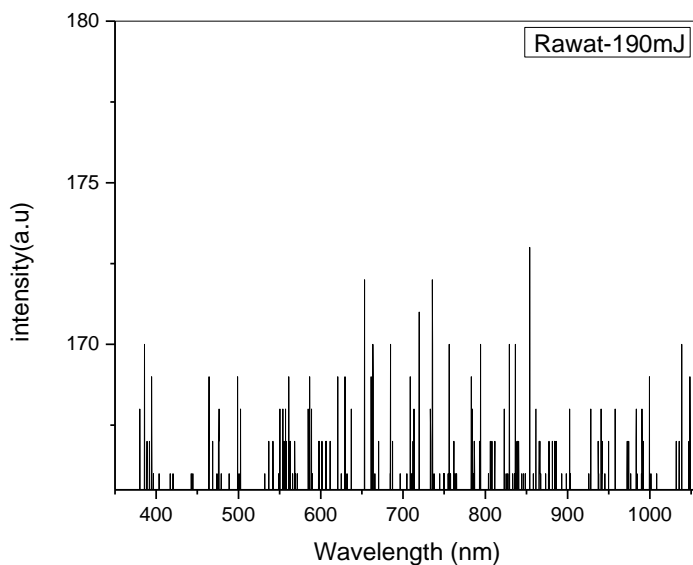
Fig (4.8): LIBS emission spectrum of Rawet oilfield irradiated with 190mJ pulse energy

Table (4.8): The data of Rawat oilfield after irradiation by 190 mJ:-

λ(nm)	Intensity (a.u)	Element
379. 78	168.041833	H I
385.48	170.030734	V I
387. 61	167.02675	C II
391. 83	167.076266	Fe I
393.94	169.056915	S II
417.54	166.01992	Ne I
419.34	166.01992	S II
441.96	166.024074	N III
443.27	166.003415	N II
463.63	169.061042	Al II
468.65	167.022624	Hg II
475	167.076266	Na VI
476.3	168.058338	Li II
486.13	166.052931	H I

λ(nm)	Intensity (a.u)	Element
498.44	169.061042	V I
533.28	166.1107	C I
553.46	168.066591	Cu II
559.79	169.044536	O V
561.76	169.044536	Kr II
563.05	167.105151	Cu II
586.49	169.056915	C I
585.2	168.041833	Na III
588.62	168.041833	Nd I
597.07	167.076266	C I
599. 52	167.076266	O I
601. 64	167.076266	C I
620.37	169.061042	Cu II
624. 07	166.057057	V I
651.93	172.09391	Mn I
660.4	169.061042	Ar I
663. 00	170.0348861	V II
670. 02	167.030876	S IV
684.82	170.034861	Si III
696.71	166.036426	Na II
711.51	167.055635	C I
713.12	168.074843	Fe II
710. 70	166.069437	S V
711.51	167.076266	C I
713.29	168.041833	Fe I
720.14	171.012806	Gd II
733.16	168.041833	Cu II
754.53	166.052931	O III
765.08	170.076124	Hg I
784.88	168.041833	Si II
805.1	167.014371	Cl I
826.79	166.057057	H I
839.93	167.018497	V II
841.24	166.457314	Kr I

λ(nm)	Intensity (a.u)	Element
828.86	170.35259	Hg I
843.35	166.028173	Co II
847.59	166.028173	Nb I
850.24	166.094195	H I
859.83	168.083096	H I
866.5	167.109277	H I
880.94	167.035033	Ni I
885.51	167.035003	S IV
891.86	166.048805	C I
901.53	168.087223	H I
925.39	166.048805	Hg I
928.64	168.087223	V II
938.08	167.068014	Cl II
941.34	168.087223	S I
946.54	166.048805	Fe II
950.13	167.07214	Fe II
976.33	166.085942	Fe I
982.68	168.070717	Fe I
984.47	166.032299	Fe II
990	168.066591	Na VIII
991.64	167.063887	C u II
999.94	169.036283	Th I
1001.08	166.052931	O III
1030.65	167.018497	S II
1031.18	167.035003	3 He I
1038.21	170.051366	C I
1047.96	169.04041	K I
1048.11	169.015652	Th I
1054.29	171.025185	Cm I
1056.4	171.025185	S V

SAMPLE (3):- Melut oilfield:

4.2.9 Irradiation of Melut with 120 mJ:
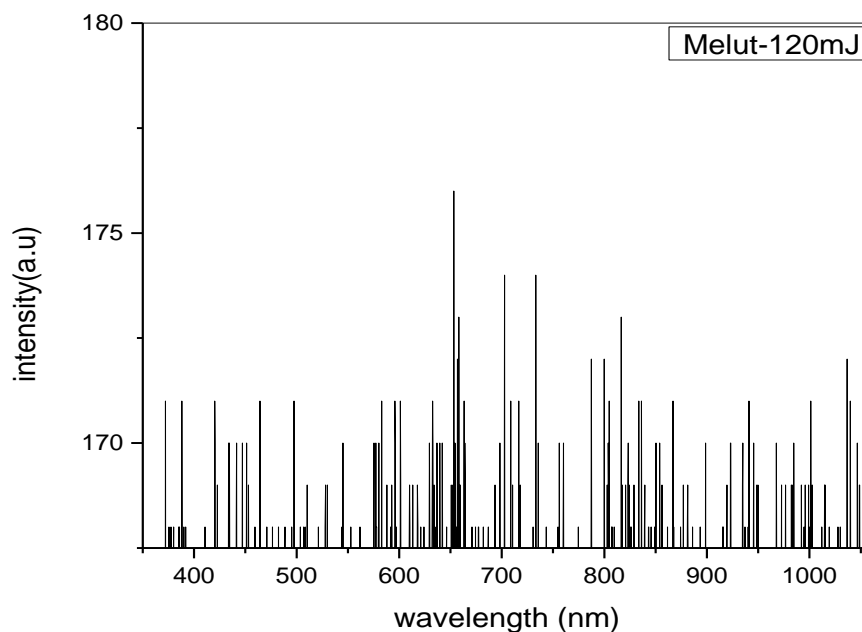
Fig (4.9): LIBS emission spectrum of Melut oilfield irradiated with 120mJ pulse energy

Table (4.9): The data Melut oilfield after irradiation by 120 mJ:-

λ(nm)	Intensity (a.u)	Element
371.81	171.042686	V II
420.48	171.042686	Na II
422.59	169.044963	Fe I
435.30	170.066022	S IV
440.66	168.751281	V I
441.64	170.021628	S IV
447.83	170.048947	C I
453.03	169.082527	S IV
545.32	170.048947	Ni I

λ(nm)	Intensity (a.u)	Element
574.94	170.021628	Ce III
593.50	168.549801	Kr III
634.68	169.075697	N II
638.43	170.035287	N II
641.03	170.052362	Br I
652.26	176.028458	C I
654.37	174.075128	O V
656.79	172.070575	Cu II
659.58	169.103017	N I
663.82	171.056346	Ar II
665.27	169.239613	Cs III
716.07	171.032442	Th II
719.32	174.051224	Mg I
755.95	170.021628	Fe I
787.69	172.101309	Fe II
804.61	171.08025	Mg II
816.49	173.050655	Nd I
824.81	169.072282	Fe I
8333.26	171.049516	S VI
835.60	171.059761	W I
835.38	171.049516	Cu II
838.63	168.546386	Ti I
839.58	169.051793	Sr III
851.04	848.888125	C I
867.12	171.08025	Al II
877.04	169.062038	S IV
920.17	169.027319	Ne I
934.48	170.066022	Ar II
941.34	168.59479	S I
946.06	170.048947	N I
948.18	169.072282	P I
950.31	169.072282	Mg I
975.69	169.072282	S IV
982.68	169.060715	Fe I

λ(nm)	Intensity (a.u)	Element
984.80	170.070575	Cr II
991.48	169.038133	Co II
999.77	169.055208	N I
993.62	168.046955	O II
993.74	168.072709	Tl I
999.77	169.050939	N I
1001.08	171.018071	O II
1012.30	168.044252	Th I
1014.42	169.061611	C II
1018.65	168.090495	Bk I
1027.11	168.044252	Th I
1036.92	172.088788	Si III
1048.60	169.058054	Fe II
1054.80	175.051935	C I
1055.60	175.030592	Si III

4.2.10 Irradiation of Melut with 150 mJ:
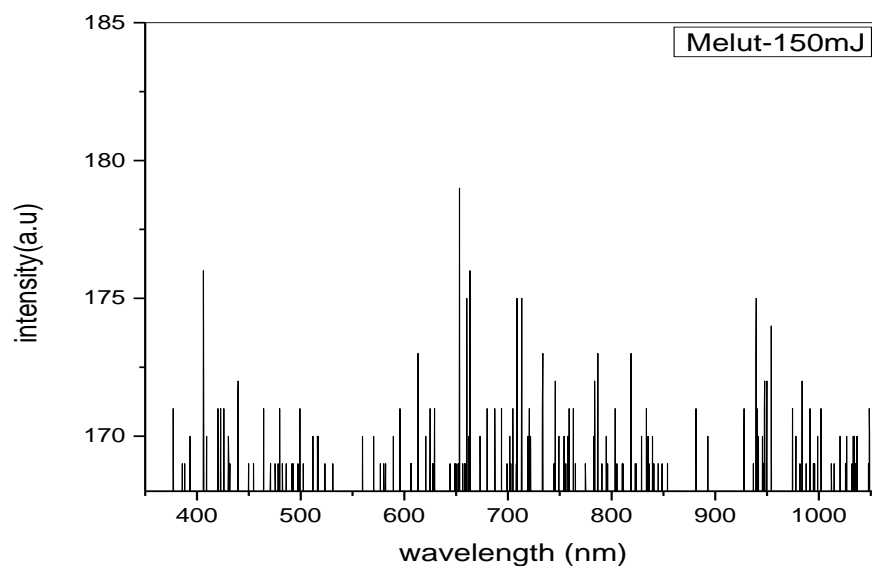
Fig (4.10): LIBS emission spectrum of Melut oilfield irradiated with 150mJ pulse energy

Table (4.10): The data Melut oilfield after irradiation by 150 mJ:-

λ(nm)	Intensity (a.u)	Element
377.19	171.06716	Cu I
385.63	169.054639	Fe I
406.15	176.098463	V I
423.09	171.06716	Cu I
425.37	170.999431	Co II
431.71	169.048901	O II
432.35	169.020774	Fe III
439.35	172.078258	U I
449.94	169.059476	Na II
463.93	171.047809	Al II
470.29	169.098179	Fe I
474.51	169.035287	Hg I
475.03	169.035287	Hg I
476.83	172.049232	N I
479.23	171.047809	Si I
480.54	169.838361	Si I
481.84	169.064314	Cl I
491.6	169.059476	198Hg I
491.6	169.059476	198Hg I
492.91	169.064314	Ba III
496.98	169.015936	Cu II
497.63	169.069152	Ni I
499.74	171.018782	Ne I
501.85	169.069152	Pr I
512.44	170.012521	Cu II
516.67	170.012521	V I
523.02	169.069152	Co I
531.48	169.006261	Co II
560.46	169.262664	V I
579.66	169.20774	Fe I
582.76	168.991747	Fe II
606.2	169.059476	C I
607.17	169.044963	Nd I

λ(nm)	Intensity (a.u)	Element
621.01	170.017359	Ne III
625.24	171.02362	Li II
627.35	169.07399	Cs II
629.48	171.02362	Ca III
648.5	169.07399	O II
650.63	169.07399	N I
651.93	179.059192	Mn I
657.47	169.020774	Nb I
658.28	169.059476	C II
659.58	175.058338	N I
660.88	175.058338	Fe I
662.35	170.03671	V I
663.66	176.054923	W I
686.61	171.018782	Fe II
702.23	170.022197	C I
705.16	171.057474	S IV
707.27	169.054639	Ti III
709.39	175.029311	Fe II
713.62	175.029311	V II
718.83	170.041548	Cs II
745.36	171.042971	V I
748.94	170.03671	Cl I
753.83	170.03671	N I
754.48	170.060899	Sc I
755.29	169.093341	Dy I
756.59	170.060899	Cr I
762.78	171.042971	Si III
783.94	172.049232	O III
786.05	173.055492	Cu II
787.68	169.054639	Fe II
788.17	169.03045	S IV
794.03	170.06309	Ar II
795.82	169.103017	V I
802.17	171.052647	Fe I
802.82	171.028458	C I

λ(nm)	Intensity (a.u)	Element
803.48	171.033295	S IV
804.28	171.052647	Fe II
809.17	169.015936	Co II
811.28	169.015936	W I
817.63	171.028458	Fe II
817.96	171.06716	Fe II
819.75	173.040979	Hg I
822.03	169.064314	Fe I
823.33	169.064314	O I
828.86	170.022197	Hg I
λ(nm)	Intensity (a.u)	Element
833.09	171.028458	B II
834.4	168.812749	Fe V
835.21	170.022197	V II
841.23	169.054639	Ti I
847.58	169.054639	Nb I
853.93	169.11753	Ti I
881.44	171.018782	Fe II
927.99	171.081673	Kr I
940.69	171.018782	Th I
941.82	170.060899	Fe II
946.06	170.060899	N I
981.21	169.112692	Fe II
981.7	169.0813665	Th II
984.47	172.068583	Fe II
991.5	170.999431	Cu II
987.24	168.98691	Co II
1012.14	169.059476	Cs II
1025.81	169.044963	Th III
1032.66	170.046386	Ar II
1047.96	171.042971	K I
1055.6	170.071998	Si III
1054.8	171.028458	C I
1055.93	171.047809	C I

4.2.11 Irradiation of Melut with 170 mJ:
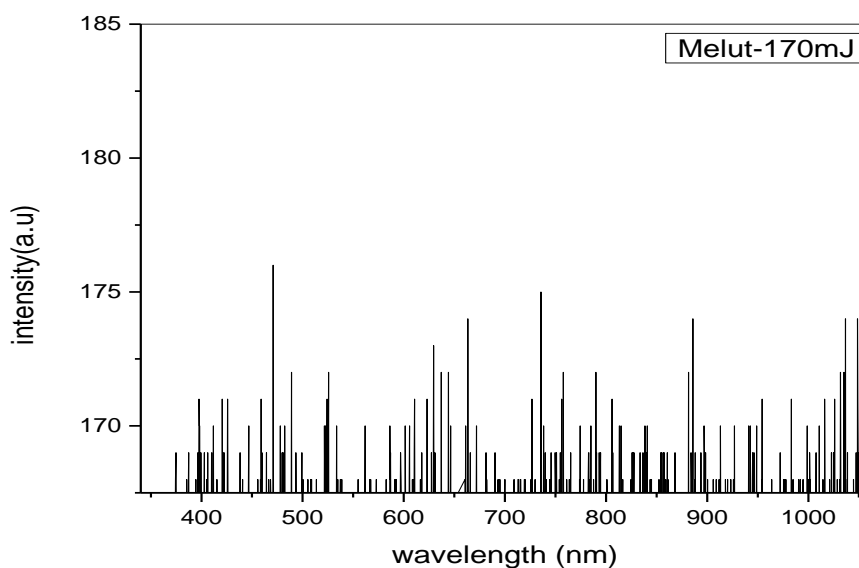
Fig (4.11): LIBS emission spectrum of Melut oilfield irradiated with 170mJ pulse energy

Table (4.11): The data Melut oilfield after irradiation by 170 mJ:-

λ(nm)	Intensity (a.u)	Element
374.66	169.035287	O V
387.53	169.035287	V I
388.90	169.083665	H I
396.94	171.028458	Fe III
406.67	169.015936	C I
405.36	168.103301	Cu II
410.17	169.020774	H I
412.31	170.089926	N II
415.26	168.157371	S I
421.71	169.103017	S II
434.04	167.032726	H I
437.36	169.044963	Fe II
445.99	168.6144	N II
477.99	170.08025	Na III

λ(nm)	Intensity (a.u)	Element
479.26	169.12066	C I
481.45	170.017359	Ni I
479.29	169.044963	V I
480.86	169.07399	C I
493.02	169.088503	O V
499.95	169.059476	Cu II
521.89	170.056061	Hg I
585.77	168.575697	Ni I
586.93	170.08025	V II
600.84	170.065737	N I
596.03	169.098179	S I
610.52	171.062322	Mn II
616.97	169.1129692	Fe III
28.69	171.720262	S II
637.11	172.068583	Ce II
660.57	170.060899	C I
672.26	170.065737	N I
681.84	169.059476	Si II
726.91	171.071998	Hg I
737.15	170.114542	Hg I
740.43	169.054639	Cu II
745.54	169.025612	O III
754.14	169.025612	K I
756.29	171.038133	Hf I
757.90	172.044394	Cu II
758.64	168.6144	C III
765.67	168.991747	O II
774.27	170.060899	Si I
782.22	108.991747	Hg I
784.33	168.362834	Ca II
785.19	170.109277	Fe II
792.88	169.078828	S I
795.13	169.078828	C I
793.62	169.088503	V I
812.62	170.056061	Li I

λ(nm)	Intensity (a.u)	Element
824.99	168.964143	H I
825.22	169.049801	H I
825.49	169.098606	H I
839.74	170.056061	C III
854.53	169.049801	H I
857.70	169.049801	C I
867.03	169.059476	Fe II
886.35	174.027888	V I
837.44	170.0249	H I
942.14	170.056061	O II
942.98	170.085088	Mg I
954.19	171.076836	Fe I
998..09	170.041548	Hg I
1007.18	169.059476	Fe I
1011.47	170.065737	Th I
1026.82	169.848036	Ar II
1047.96	169.059476	K I
1049.09	174.052077	Fe II
1051.24	170.089926	Cl II
1051.92	170.060899	Li II

4.2.12 Irradiation of Melut with 190 mJ:
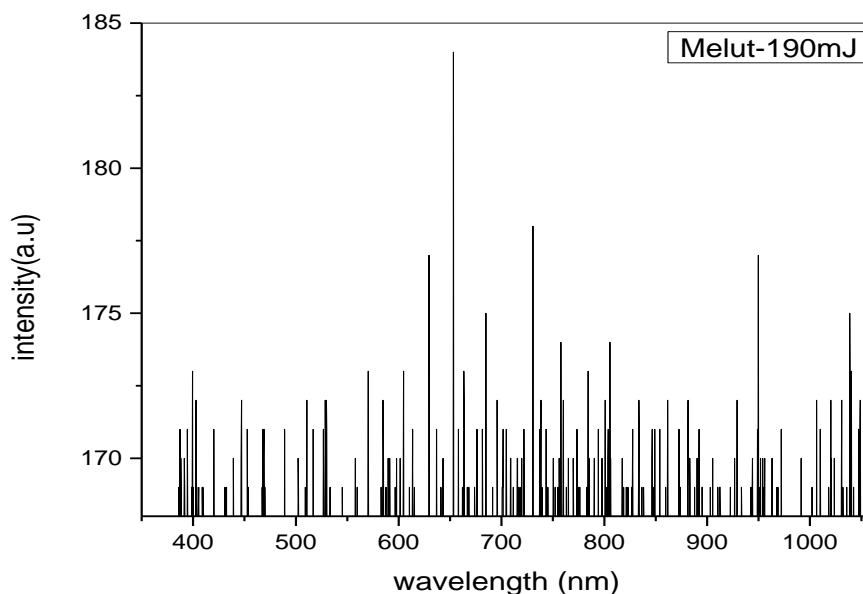
Fig (4.12): LIBS emission spectrum of Melut oilfield irradiated with 190mJ pulse energy

Table (4.12): The data Melut oilfield after irradiation by 190 mJ:-

λ(nm)	Intensity (a.u)	Element
386.95	171.04439	Fe I
388.90	170.2508	H I
390.36	170.05179	Hg I
391.18	170.03813	O III
393.30	170.9852	Cu
392.47	109.61013	V I
419.83	171.04439	Fe I
453.03	171.08082	S IV
397.01	168.71599	H I
397.00	168.61924	H I
410.17	169.09818	H I
439.19	170.07541	Ne II
528.24	172.11212	N III
530.34	172.037	Th I

λ(nm)	Intensity (a.u)	Element
585.20	172.037	Na III
589.43	170.02447	S I
597.25	170.0609	C I
601.64	170.03813	Ba III
612.22	170.03813	Ca I
629.15	177.02277	Si III
637.45	171.04439	V I
652.11	183.99829	N I
658.76	171.07627	C I
656.28	171.07627	H I
700.92	171.03529	Hg I
702.22	171.03529	C I
705.16	171.03529	S IV
715.42	170.05635	Hg I
79.65	170.05635	Th I
743.88	171.04439	Ne I
736.61	171.58054	N I
738.04	172.07797	Ar II
757.25	174.08139	Fe II
774.00	171.08537	Na VII
794.52	171.08537	Fe II
806.23	169.34149	C II
833.11	172.72453	V I
849.53	171.01708	Ne I
889.74	170.08822	Ba II
891.86	171.03529	C I
904.44	170.04269	Kr I
944.61	170.07911	V II
948.83	171.08537	O IV
955.33	170.03813	3He I
991.63	170.03813	Kr I
1006.45	172.05066	Fe II
1022.98	170.03358	Fe I
1038.21	175.04212	C I
1040.30	173.08879	Th I

λ(nm)	Intensity (a.u)	Element
1047.96	171.0535	K I
1048.60	172.0461	Fe II

National institute standard technology-Atomic spectra database (NIST ASD) was used for the spectral analysis of the elements in the three samples. Tables (4.1) to (4.12) list the analyzed data for the three samples.

4.3 The Quantitative results:

Table (4.13): The analyzed data of main elements in three crude oil samples collected from three different areas, after irradiation by 120 mJ:-

Element	Melut-120mJ λ(nm)	Melut-120mJ intensity	Rawat-120Mj λ(nm)	Rawat-120Mj Intensity	Hadida-120mJ λ(nm)	Hadida-120mJ intensity
C I	652.26	176.028458	702.22	702.232921	594.01	164.054069
	851.04	848.888125	887.33	170.060899	606.198991	163.055208
			994.13	170.041548		
			1044.99	169.02774		
C II			652.26	181.062038		
C III			835.87	169.020794	835.87	163.08082
H I		---			850.22	162.97325
N I	659.58	169.103017	946.06	176.074274		---
	946.06	170.048947	---	---		
	999.77	169.055208	---	---		
N II	634.68	169.075697	499.43	169.084804	470.94	163.516221
	638.43	170.035287			554.34	164.079681
					867.6	164.525327
N V		---	732.65	173.040979		---
N IV		---	937.82	169.044963	520.42	163.101309
O II	993.62	168.046955	428.13	167.993739	428.13	163.039841
					541.91	165.052931
					722.91	164.084804
O III		---	719.02	170.044394		---
			968.85	169.059476		
O V	654.37	174.075128		---		---
O IV		---	415.75	169.059192		---
S I	941.34	168.59479		---		---

Element	Melut-120mJ		Rawat- 120mJ		Hadida- 120mJ	
	λ(nm)	Intensity	λ(nm)	intensity	λ(nm)	intensity
S II	----		970.1	168.619237	393.94	165.073421
					547.93	163.085942
					547.93	163.06033
S IV	435.3	170.066022	---		647.87	163.009106
	441.64	170.021628				
	453.03	169.082527				
	877.04	169.062038				
	975.69	169.072282				
S VI	8333.26	171.049516	---		---	
S V	---		---		865.5	164.12583

Table (4.14): The analyzed data of main elements in three crude oil samples collected from three different areas, after irradiation by 150 mJ:-

Element	Melut-150mJ		Rawat- 150mJ		Hadida- 150mJ	
	λ(nm)	Intensity	λ(nm)	intensity	λ(nm)	intensity
C I	606.2	169.059476	421.3	168.10359	---	
	702.23	170.022197	697.02	167.07228		
	802.82	171.028458	601.64	171.02675		
			611.58	166.68981		
			665.93	169.08025		
C II	658.28	169.059476	---		---	
C III	---		425.53	17103358	759.53	165.060899
			835.87	170.07359	850.03	167.083096

	Melut-150mJ		Rawat- 150mJ		Hadida- 150mJ	
Element	λ(nm)	Intensity	λ(nm)	Element	λ(nm)	Intensity
H I	---		835.87	170.07359	850.03	167.083096
					833.09	164.001423
					837.44	165.070058
N I	476.83	172.049232	623.76	168.04212	646.06	168.55492
	650.63	169.07399				
	659.58	175.058338				
	753.83	170.03671				
	946.06	170.060899				
N II	---		650.46	167.12692	860.43	164.064314
N IV	---		918.21	168.9963	---	
O I	823.33	169.064314	---		---	
O II	431.71	169.048901	---		964.84	164.064314
	648.5	169.07399				
O III	783.94	172.049232	391.18	167.0313	755.14	166.018782
			736.53	168.36312		
O IV	---		715.9	169.05293	---	
S I	---		605.26	173.068867	815.34	164.088503
					864.84	164.064314
S IV	705.16	171.057474	---		---	
	788.17	169.03045				
	803.48	171.033295				

Table (4.15): The analyzed data of main elements in three crude oil samples collected from three different areas, after irradiation by 170 mJ:-

element	Melut-170mJ λ(nm)	Melut-170mJ intensity	Rawat-170mJ λ(nm)	Rawat-170mJ intensity	Hadida-170mJ λ(nm)	Hadida-170mJ intensity
C I	406.67	169.015936			601.63	163.566022
	479.26	169.12066			702.22	164.035287
	480.86	169.07399	543.68	167.05976	721.6	166.06718
	660.57	170.060899				
	795.13	169.078828				
	857.7	169.049801				
C II	---		652.26	175.05179	---	
C III	758.64	168.6144	835.87	169.05478	425.21	167.083096
	839.74	170.056061				
H I	388.9	169.083665	486.12	167.08307	486.07	164.040125
	410.17	169.020774	824.99	166.05706	486.12	165.065737
	434.04	167.032726	828.64	168.12023	656.27	164.044963
	824.99	168.964143	486.12	167.08307	486.07	164.040125
	825.22	169.049801	824.99	166.05706	486.12	165.065737
	825.49	169.098606	828.64	168.12023	656.27	164.044963
	854.53	169.049801				
	837.44	170.0249				
N I	600.84	170.065737	536.7	167.03017	661.05	163.977234
	672.26	170.065737				

Element	Melut-170mJ λ(nm)	Intensity	Rawat- 170mJ λ(nm)	Element	Hadida- 170mJ λ(nm)	Intensity
N II	412.31	170.089926	718.81	167.79852	470.94	164.064314
	445.99	168.6144			700.09	164.054639
					754.53	166.062322
N V	---		---		654.7	166.81218
O I	---		747.64	168.04439	---	
O II	765.67	168.991747	419.67	172.05137	469.63	164.06314
	942.14	170.056061	431.71	169.04326		
O III	745.54	169.025612	---		755.14	166.0623
O V	374.66	169.035287	654.37	172.036	---	
	493.02	169.088503				
S I	415.26	168.157371	---		587.96	164.098179
	596.03	169.098179				
	792.88	169.078828				
S II	421.71	169.103017	393.94	171.02177	684.82	164.054639
	28.69	171.720262	547.93	167.05976		
			727.32	169.01252		
S IV	---		---		885.51	166.038133

Table (4.16): The analyzed data of main elements in three crude oil samples collected from three different areas, after irradiation by 190 mJ:-

element	Melut-190mJ λ(nm)	Intensity	Rawat-190mJ λ(nm)	intensity	Hadida-190mJ λ(nm)	Intensity
C I	597.25	170.060899	533.28	166.1107	525. 96	165.057769
	658.76	171.076266	586.49	169.056915	601.641449	169.085657
	702.22	171.035287	597.07	167.076266	722.416323	166.025896
	891.86	171.035287	601. 64	167.076266	802.824392	165.081673
			711.51	167.055635		
			711.51	167.076266		
			891.86	166.048805		
C II	806.23	169.341491	387. 61	167.02675	675.050436	165.003984
H I	388.9	170.250802	379. 78	168.041833	387.394	164.02675
	397.01	168.715993	486.13	166.052931	652.262724	180.063745
	397	168.619237	826.79	166.057057	835	168.069721
	410.17	169.098179	850.24	166.094195	837. 44	168.069721
	656.28	171.076266	859.83	168.083096	886. 28	165.057769
			866.5	167.109277		
			901.53	168.087223		
N I	652.11	183.998293			672.93434	165.003984
	736.61	171.58054		---	690.025218	166.09761
					946.06144	168.039841
N II	---		443.27	166.003415	568. 62	167.02988
N III	528.24	172.112123	441.96	166.024074	838.633654	165.111554

	Melut-190Mj		Rawat- 190mJ		Hadida- 190mJ	
Element	λ(nm)	Intensity	λ(nm)	Element	λ(nm)	Intensity
O I	---		599. 52	167.076266	615.802384	166.109562
					702. 55	165.087649
O II	---		---		410.875745	165.063745
O III	391.18	170.038133	754.53	166.052931	---	
O V	---		559.79	169.044536	---	
O IV	948.83	171.085373	---		576. 91	166.01992
					783.780376	166.047809
					853.445667	167.053785
S I	589.43	170.024474	941.34	168.087223	54. 98	165.111554
					587.968822	166.115538
S II	---		393.94	169.056915	668. 18	164.139442
			419.34	166.01992		
S IV	453.03	171.08082	670. 02	167.030876	696.373223	166.01992
	705.16	171.035287	885.51	167.035003	---	

4.4 Discussion:

The LIBS spectra of the crude oil samples were recorded to identify each element present in the sample. The most sensitive lines (finger print wavelength) for identification of elements were found between (200-1100) nm regions using NIST database.

The wavelengths for all these elements are indicated on the spectrum samples which investigated by (120mJ, 150 mJ, 170mj and 190 mJ).

Since the interaction between focused laser pulses and the sample creates plasma composed of ionized matter, so when pulse energy was increased we notes that some ions were appeared at higher order ionization stage because with higher energy supply it is possible to detached more electrons overcoming the second ionization potential, the third, and so on.

The identification of each spectral line is listed in table 4.1 to 4.12.

The main elements in crude oil sample (C, H, O, N and S) and heavy elements like (Fe, Cu, Ni and V) were detected by using LIBS techniques.

At pulse energy 190mJ the Carbon ions C II appeared in all samples because this energy was sufficient to ionized carbon atoms.

Sulfur ions when irradiated by 190mJ were detected with higher amount in Rawat oilfield than Hadida and Melut.

Also Rawat 150mJ showed higher amount of Carbon element.

Hydrogen and Carbon founded with higher amount and ionization in Melut oil field than Rawat and Hadida.

At 120mJ nitrogen ions appeared higher in Melut oilfield and Carbon ions detected with higher amount in Rawat. Also Oxygen was higher in Hadida oilfield. Sulfur was higher in Melut. This variety is due to the location, age and depth of the field.

When pulse energy increased to 150mJ the number of elements detected was increased with different ionization stages. Carbon ions C I, C II and C III were detected in Melut oilfield. Nitrogen N II and N IV in Rawat oilfield were founded. Oxygen ions O I, O II and O III in Melut were detected.

Sulfur with higher ionization S IV detected in Melut and disappeared in Hadida and Rawat.

At 190 mJ the amount of nitrogen ions N I, N II and N III increased in Hadida, also Sulfer S I, S II and S IV in Rawat oilfield. Oxygen with little amount in Melut was appeared. Carbon and Hydrogen with higher ionization and amount in Rawat

 These results demonstrate that the amount of different atoms and ions of metals appeared in all three samples depend on the power of the laser, locations of the samples which were collected from. And also the ionization of neutral atoms depends on the laser power.

Finally, LIBS techniques can provide an easy, fast, and in situ analysis with a reasonable precision, detection limits, and cost. Additionally, there is no need for sample preparation.

4.5 Conclusion:

The spectra due to main elements in crude oil such as C, H, O, N, and S were recorded using LIBS technique. Also trace elements such as Ni, V, Cu, Fe, was appeared.

The amount of heavy metals in crude oil samples was increased by increasing the power density of laser.

New elements are not detected previously were found in this work which is: Ho, Gd, Bk, Hf which reveals the advantage of used LIBS technique.

Measurements also shows trace elements like Hg, Mn, Ca, Co, Th.., etc as shown in table (4.1 to 4.12).

The results show good agreement with Dr. Saif aldeen [15].

The LIBS technique proved to be efficient in detection of elements in crude oil samples even those with little amounts. Also LIBS is good and fast technique that can be used for the detection of elements in flammable and hazard materials.

4.6 Recommendation:

1. Increased the pulse energy up to 190mJ and study the physical and optical properties of crude oil samples.

2. Use the double pulses to improving sensitivity and reducing ambient interferences.

3. Coupled LIBS with other spectroscopic devices like Raman and ICP for additional measurement capabilities.

References:-

1. Dr. Mircea Gheorghiu-Prof. Andrei Tokmakoff-Lecture Notes: Introduction to Spectroscopy-MIT open course-2007.

2. Introduction to Spectroscopy and Applications-Ocean Optics-2017.

3. F. Anabitarte, A. Cobo, and J. M. Lopez-Higuera-Laser-Induced Breakdown Spectroscopy: Fundamentals, Applications, and Challenges-ISRN Spectroscopy-2012.

4. J. M. Vadillo -J. M. Fernández Romero -C. Rodríguez -J. J. Laserna-Effect of plasma shielding on laser ablation rate of pure metals at reduced pressure-wiley online library. -1999.

5. Bala Kunjappa – An Introduction to Energy Sources - -2006.

   Norman, J. Hyne (20 Nontechnical guide to petroleum geology, exploration, drilling, and production . Tulsa, OK: Penn Well Corp-2006.

   7. Singh, Jagdish, and Surya Narayan Thakur - Laser-induced breakdown spectroscopy-Elsevier -2007.

8. Robert Curley, Adam Augustyn, Patricia Bauer- Crude Oil Petroleum Product-Britanica-2017.

9. F. Anabitarte, A. Cobo, and J. M. Lopez-Higuera- Laser-Induced Breakdown Spectroscopy: Fundamentals, Applications, and Challenges-ISRN Spectroscopy- Hindawi Publishing Corporation-2012.

10. David W. Hahn-Laser-Induced Breakdown Spectroscopy (LIBS), Part II: Review of Instrumental and Methodological Approaches to Material Analysis and Applications to Different Fields-ResearchGate-2012.

11. Mikko Jarvikivi- What is LIBS-Hitachi High Technique -2018.

12. David A. Cremers, Leon J. Radziemski - Handbook of Laser-Induced Breakdown Spectroscopy-John Wiley and Sons.LTD- 2006.

13. Andrzej W. Miziolek, et al –Laser Induced Breakdown Spectroscopy (LIBS): Fundamentals and Applications- cambridge university press - 2006.

14. –Hek de Wit-Introduction, Application and advantages of LIBS-Andor technology-AZO Optics-2010.

15. Nafie A. Almuslet1 and Saifeldin Yassin Mohamed1-Laser Induced Breakdown Spectroscopy Applied to Elemental Analysis Using Samples of Crude Oil from Adaril Oilfield- British Journal of Applied Science & Technology-2013.

16. Yong He-Jiajian, et al - In-situ Measurement of Sodium and Potassium Release during Oxy-Fuel Combustion of Lignite using Laser-Induced Breakdown Spectroscopy: Effects of O_2 and CO_2 Concentration- American Chemical Society-2013.

17. Epuru Nageswara Rao, Sreedhar Sunku, Soma Venugopal Rao- Femtosecond Laser-Induced Breakdown Spectroscopy Studies of Nitropyrazoles: The Effect of Varying Nitro Groups- Society for Applied Spectroscopy- 2015.

18. M. A. Gondal- Willis Maganda- Mohamed Abdulkader Dastageer- Detection of carcinogenic chromium in synthetic hair dyes using laser induced breakdown spectroscopy-ResearchGate-2014.

- 19. Salvador Guirado- Francisco J Fortes- J Javier Laserna -Multi-Pulse Excitation for Underwater Analysis of Copper-Based Alloys Using a Novel Remote Laser-Induced Breakdown System-ResearchGate-2016.

20. Khalil AA, Gondal MA, Shemis M, Khan IS.- Detection of carcinogenic metals in kidney stones using ultraviolet laser-induced breakdown spectroscopy-PubMed-NCBI-2015.

- 21. Mauro Martínez, et al-Determination of Ni and V in Crude Oil Samples Encapsulated in Zr Xerogels by Laser-Induced Breakdown Spectroscopy-ACS Publications-2015.

22. Maria M. Ossman; Supervisor,-Nafie A. Almuslet-Utilization of Laser Induced Breakdown Spectroscopy (LIBS) to Detect the Heavy Metals and their Concentrations in Dairy Products Waste Water-SUST Repository-2015.

23. Gondal MA1, Habibullah YB2, Baig U2, Oloore LE2.-Direct spectral analysis of tea samples using 266 nm UV pulsed laser-induced breakdown spectroscopy and cross validation of LIBS results with ICP-MS- PubMed-NCBI-2016.

24. C.M.Ahamera, et al -Laser-induced breakdown spectroscopy of major and minor oxides in steel slags: Influence of detection geometry and signal normalization- Elsevier- 2016.

25. Hervé K. Sanghapi- Alexander Bolshakov - Determination of Elemental Composition of Shale Rocks by Laser Induced Breakdown Spectroscopy (LIBS) -ResearchGate-2016.

26. Tianlong-Zhanga, et al.- Classification of steel samples by laser-induced breakdown spectroscopy and random forest - Elsevier-2016 .

27. Jinmei Wang,Shuwen Xue,Peichao Zheng,Yanying Chen &Rui Peng-Determination of Lead and Copper inLigusticum wallichii by Laser-Induced Breakdown Spectroscopy-Analytical letters-Taylor Francis online-2017.

28. M. M. Nasr, M. A. Gondal, M. M. Ahmed, M. M. Yousif, and N. A. Al-Muslet- Direct spectral analysis of different gum Arabic samples using laser induced breakdown spectroscopy- AIP Publishing-2018.

29. Aissa Harhira--Josette El Haddad-Alain Blouin-Mohamad Sabsabi
- Rapid Determination of Bitumen Content in Athabasca Oil Sands by Laser-Induced Breakdown Spectroscopy- ACS Publications (American Chemical Society) -2018.

30. Senesi, G.S., Manzini, D., De Pascale, - Application of a laser-induced breakdown spectroscopy handheld instrument to the diagnostic analysis of stone monuments-PubAg-USDA-2018.

31. N. H. Thomas-B. L. Ehlmann et al. - Characterization of Hydrogen in Basaltic Materials With Laser- Induced Breakdown Spectroscopy (LIBS) for Application to MSL ChemCam Data -AGU Publications-2018.

32. M.A. Gondala,∗ , T. Hussainb, Z.H. Yamania, M.A. Baigb-Detection of heavy metals in Arabian crude oil residue using laser induced breakdown spectroscopy-Elsevier-2006.

33. Ali Ibrahim Neamah – separation of the petroleum sysrem- research gate-2014.

34. Mashair A. Mohammed Supervisor: Nafie A. Almuslet-Characterization of gum Arabic using laser Induced Breakdown Spectroscopy (LIBS) - SUST Repository-2017.

35. USB Series Spectrometers-Ocean Optics.